A. Lightbody
1-279

NOLTR 61-49

JRB 3

SOLID STATE RESEARCH OF THE APPLIED PHYSICS DEPARTMENT FOR THE YEAR 1960

29 MAY 1961

NOL

UNITED STATES NAVAL ORDNANCE LABORATORY, WHITE OAK, MARYLAND

NOLTR 61-49

SOLID STATE RESEARCH
OF
THE APPLIED PHYSICS DEPARTMENT
FOR THE YEAR 1960

L. R. Maxwell, Editor

ABSTRACT: This is a report describing the accomplishments of the Applied Physics Department for the calendar year 1960. The effort has been concentrated on investigations of the energy bands in semiconductors by optical methods dealing with the lead salt compounds Pbs, PbSe, and PbTe, as well as certain intermetallic semiconductors. This work also includes measurements of the reflectivity of intermetallic semiconductors. Investigations of the composition properties of lead telluride have resulted in a better understanding of the phase diagrams of lead telluride. We have continued work on surface effects and transport phenomena, and on the study of recombination lifetimes.

The magnetic behavior of rare earth magnetic alloys has been examined. The effect of Zener's double exchange phenomenon has been obtained in certain manganese compounds. We have carried out theoretical work on crystal and magnetic anisotropy and how it relates to the intensity of magnetization and the Curie temperature. The physical properties of materials have been studied, in particular the properties of intermetallic metals, metal oxide whiskers, and the structure of fuzed silica. In the latter instance we have been able to obtain important information as to the atomic configurations. Our neutron diffraction studies have found aspherical unpaired 3d electron charge distributions in iron, aluminum and NiO compounds.

U. S. NAVAL ORDNANCE LABORATORY
WHITE OAK, MARYLAND

THE STAFF

D. F. Bleil, Associate Director for Research

W. C. Wineland, Physics Program Chief

Applied Physics Department

L. R. Maxwell, Department Chief
W. W. Scanlon, Senior Research Physicist

Divisions

Magnetic Materials--E. Adams, Acting Chief
Physical Properties of Materials--T. R. McGuire, Acting Chief
Solid State--F. Stern, Acting Chief

Consultants

C. G. Shull
R. M. Thomson
R. J. Maurer
P. H. Miller, Jr.

Intermittent Staff

T. A. Litovitz
E. C. Treacy
R. K. Wangsness
R. A. Ferrell

Molecular Magnetism in Solids

E. R. Callen
E. S. Dayhoff
S. J. Pickart
H. A. Alperin
A. E. Clark
B. F. DeSavage
B. V. Kessler
E. P. Wenzel
J. Lamberth

Imperfections in Solids

P. L. Edwards
R. E. Strakna
R. J. Happel, Jr.
S. F. Ferebee

Absorption in Liquids

W. M. Slie
W. M. Madigosky

Semiconductors

R. S. Allgaier
F. Bis
R. F. Brebrick
J. R. Burke, Jr.
J. L. Davis
J. R. Dixon
J. Ellis
D. P. Enright
R. F. Greene
E. Gubner
B. B. Houston, Jr.
J. Jensen
M. K. Norr
H. R. Riedl
E. J. Scott
J. O. Varela
J. N. Zemel

The Applied Physics Department reports for the year 1960 on its accomplishments in basic and applied research on materials which is supported to a large extent by Foundational Research funds provided by the Bureau of Naval Weapons.

W. D. COLEMAN
Captain, USN
Commander

Louis R. Maxwell

L. R. MAXWELL
By direction

CONTENTS

ILLUSTRATIONS

TABLES

MATERIALS REPORT FOR THE APPLIED PHYSICS DEPARTMENT

INTRODUCTION

The year 1960 constituted the third anniversary of the formation of the Applied Physics Department; an effort to bring together various projects and interests that are concerned with the properties of materials. In this report we summarize briefly the various accomplishments. The plan has been one emphasizing category of endeavor rather than a formal separation of basic from applied studies. In this manner we present a well rounded program of various undertakings.

During the year we were pleased to have published the book covering the second conference on semiconductor surfaces, which was held at this Laboratory on 2, 3, and 4 December 1959. This conference was carried out under co-sponsorship of the U. S. Naval Ordnance Laboratory and the Office of Naval Research. The conference was a logical undertaking in view of the interest that had been continually present in this Laboratory on surface properties. Reports were presented on new techniques used in the study of semiconductor surfaces, the preparation of clean surfaces of germanium and silicon, the theory of surface transport noise and origin of surface states, the properties of 2-6 and 3-5 compounds, surface chemistry, and other similar problems.

During the summer of 1960 we took an active part in the Prague International Conference by presenting four papers at this meeting.

Our neutron diffraction work on magnetic materials has been shaping up along the lines of form factor investigations and in particular the asymmetrical nature of the 3d unpaired electron charge distributions in transition metal atoms. We are now carrying this as one of our primary objectives to determine not only the nature of this asymmetry but also how it will vary according to the type of atoms present, i.e., the differences between neutral atoms and ionic ones.

We now report for the first time on new work being undertaken on a class of compounds known as intermetallic metals. This general class can be identified as compounds which exhibit a melting point higher than either of the constituent elements. We present findings of a new alloy that shows extreme hardness and yet remains non-magnetic.

During the year we have emphasized to a greater extent the importance of the use of ultrasonic methods for determining the properties of

materials. This is proving to be successful in several instances.

BAND STRUCTURE OF THE LEAD SALT SEMICONDUCTORS PbS, PbSe, and PbTe

Weak-field magnetoresistance in a cubically-symmetric crystal may be expressed in terms of three coefficients b, c, and d from which, under favorable circumstances, information concerning the band structure and scattering mechanisms in the material may be deduced. When the energy band extrema are ellipsoids of revolution located along symmetry axes, these coefficients are a function of two parameters: G, a combination of integrals depending on the scattering law and the statistics, and K, the anisotropy parameter (the ratio of mass anisotropy to scattering time anisotropy). In this type of model, a relationship of the form $b + c + xd = 0$ exists among the coefficients, independently of the values of G and K. For energy surfaces which are ellipsoids of revolution along the $\langle 100 \rangle$, $\langle 111 \rangle$, or $\langle 110 \rangle$ directions in k-space x equals 1, 0, or -1, respectively.

Recently, we obtained magnetoresistance data on high-quality single crystals of p-PbTe which were grown at NOL using the Czochralski method. We found that $x = 0 \pm 0.03$ at room temperature and at 77°K, a strong indication that $\langle 111 \rangle$ valleys are present in the valence band of PbTe. The formulas for this model then lead to the values G = 1.17, K = 4.74 (room temperature), and G = 1.016 and K = 4.20 (77°K). Preliminary room temperature results for n-PbTe also suggest $\langle 111 \rangle$ ellipsoids with somewhat smaller anisotropy ($K \approx 3$), while for n- and p-type PbS and PbSe the longitudinal magnetoresistance coefficients are an order-of-magnitude smaller than in p-PbTe. This suggests approximately spherical energy surfaces centered at k = 0 for these bands, rather than multiple ellipsoids.

OPTICAL ABSORPTION IN THE LEAD SALTS

It has been shown theoretically that the absorption coefficient in semiconductors caused by optically induced transitions across the forbidden energy gap should be proportional to $(h\nu - E_G)^{1/2}$ for allowed direct transitions and proportional to $(h\nu - E_G)^2$ for some indirect transitions. Here $h\nu$ is the photon energy, and E_G is the optical energy gap. This theory has been applied experimentally to the lead salts, and the values for direct and indirect transition energies obtained. One would also like to know whether the indirect transitions are vertical transitions (no change in crystal momentum) or not.

One possible method to distinguish between a vertical and a non-vertical indirect transition is to observe the energy dependence of the absorption near the edge as a function of temperature below the Debye temperature. This has been done but the results were not decisive enough to be able to distinguish between the two models. This experiment, however, did show good agreement with the rate of change of indirect transition energies with respect to temperature found by Gibson.

Another possible method to explore the band structure is optically to induce transitions from one minimum to another within the conduction band or the valence band. This is being attempted on n-type and p-type material. In p-type PbS, preliminary experiments indicate that there may be absorption at energies smaller than the energy gap but much larger than the energy difference between direct and indirect transition energies.

STARK SPLITTING OF THE DIRECT EXCITON IN GERMANIUM

A study of strong internal electric fields has been begun using the Stark splitting of the exciton line in germanium as a measuring tool. An extremely thin diode structure will be employed and biasing of the diode will give the internal fields. No measurements have been made yet since instrumentation for the experiment has not been completed.

SHIFT OF THE FUNDAMENTAL ABSORPTION EDGE OF INDIUM ARSENIDE TO LOWER ENERGIES

The absorption of infrared light in indium arsenide at room temperature increases very abruptly in the neighborhood of four microns. This is often referred to as the fundamental absorption edge region. The rapid change in the absorption is due to the onset of photon-induced electronic transitions between the valence and the conduction bands. Thus, the position of the absorption edge serves as a measure of the separation of these bands. A topic of particular interest has been the dependence of the position of the edge upon the concentration of impurities. Previous studies at this Laboratory have shown that the addition of donor impurities to InAs moves the edge to higher energies. This is related to the filling of energy levels near the bottom of the conduction band. In contrast to this, recent studies have shown that the addition of acceptor impurities moves the absorption edge to lower energies. Similar negative shifts have been reported in indium antimonide, gallium arsenide, and cadmium telluride. Consequently, the phenomenon appears to have fundamental significance.

Our experimental results applying to this negative shift are presented in Fig. 1. The data represented by the squares apply to relatively pure InAs, with a net donor concentration of 2×10^{16} per cm^3. The other two sets of data apply to materials with the zinc-acceptor impurity concentrations indicated in Fig.1. The magnitude of the shift increases with the number of acceptors. For an acceptor concentration of $2.4 \times 10^{17} cm^{-3}$, the shift measured at an absorption coefficient of 100 cm^{-1} is 0.013 ev. D. M. Eagles of the Services Electronics Research Laboratory in England has proposed that this shift is due to electronic transitions between the added acceptor levels and the conduction band. His theory indicates that the absorption coefficients at a given low energy such as 0.34 ev in the figure should be proportional to the acceptor concentration. This prediction is substantiated by the experimental results. On the other hand, the theoretical energy dependence of the absorption coefficient associated with transitions of this type is considerably weaker than found experimentally. It is possible that the discrepancy is due to transitions originating from other levels which have not been taken into account. Another possibility is that the discrepancy is due to a failure of some of the simplifying assumptions on which Eagles' theory is based. These points require further study.

CALCULATIONS OF OPTICAL ABSORPTION OF INTERMETALLIC SEMICONDUCTORS

General features of the electronic energy band structure of III-V intermetallic semiconductors such as indium arsenide are fairly well known, but not all of the parameters which enter have been accurately evaluated. One useful method for determining these parameters is through optical measurements, which can then be compared with calculations based on specific models.

Calculations have been made for both indium arsenide and indium antimonide. For InAs the calculated absorption beyond the intrinsic absorption edge was compared with experimental values determined at NOL. The effective mass at the bottom of the conduction band was found to be 0.024 ± 0.003 times the free electron mass. Coulomb interaction between the electron and hole produced by absorption of a photon has not been considered as yet, and will probably lead to an adjustment of the estimated mass. Calculations have also been made for the interband transitions in InSb. When these are compared with published data, a value of 0.4 ± 0.1 times the free electron mass is deduced for the average effective mass of heavy holes. This is about twice as big as the usually quoted value, but seems to be consistent with a fairly wide range of observations. Calculations similar to these can be made for other III-V semiconductors as

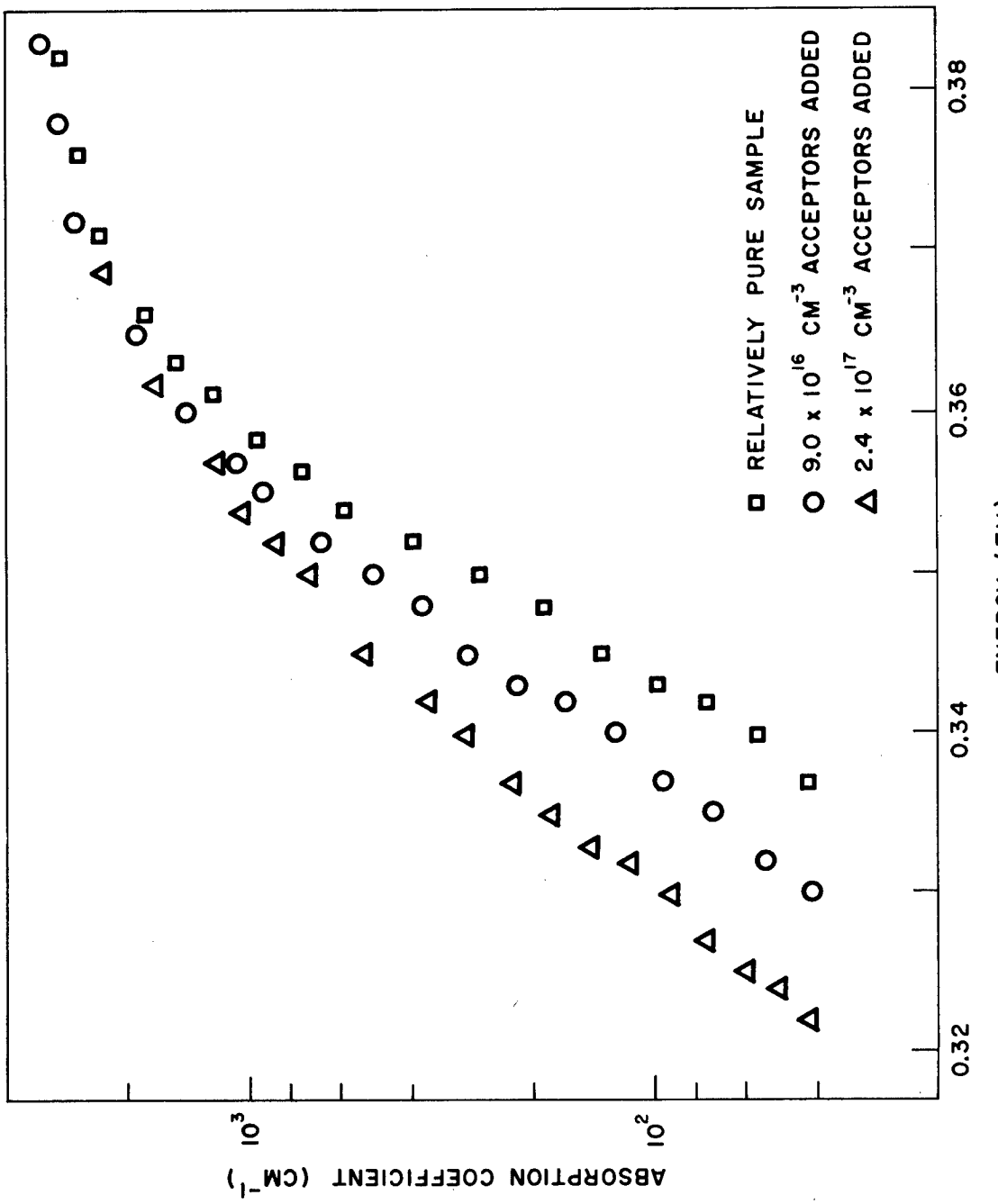

Fig. 1. The shift in the position of the fundamental absorption edge of indium arsenide at room temperature as a function of zinc-acceptor concentration.

suitable optical absorption data become available, and should help to give more accurate values of band structure parameters, particularly for the heavy holes.

REFLECTIVITY OF INTERMETALLIC SEMICONDUCTORS

Information about the optical properties of semiconductors is normally obtained from measurements of absorption constant and reflectivity. For energies well above the intrinsic energy gap, however, the optical absorption becomes so strong that extremely thin samples are required if light is to be transmitted through them. A form of the Kramers-Kronig relations, based on the requirement that no effect can precede the source of the effect, gives the phase of the complex reflectivity if its magnitude is known over a sufficiently wide frequency range. Thus, reflectivity measurements can be used to give the optical constants in the frequency range for which absorption measurements are difficult.

The reflectivities of polished samples of several intermetallic semiconductors are to be measured at normal incidence over the spectral region from 2200 Angstroms to 15 microns for a number of samples of indium antimonide, indium arsenide, and gallium arsenide. A Perkin Elmer model 112U spectrometer equipped with reflectance attachment is employed for obtaining relative reflectivity data. A rhodium mirror, recently calibrated outside the Laboratory, is used as a secondary standard for conversion to absolute reflectance in the visible and ultraviolet regions, while an aluminized mirror serves this purpose in the infrared. The calculation of the optical constants as outlined above is being programmed for machine computation.

CHEMISTRY OF THE PbS DEPOSITION REACTION

Sensitive infrared detectors of PbS can be prepared either by evaporation or by chemical deposition. During the past several years an effort has been made at this Laboratory to correlate the chemistry of the aqueous deposition of PbS films with their physical properties. As a part of this project, a kinetic study of the deposition reaction was undertaken.

The solution used for depositing the films was prepared by mixing together solutions of sodium hydroxide, a lead salt, and thiourea. It was found that within the experimental error, the molar ratio of the lead to hydroxide consumed during the reaction was 1:2, and the ratio of thiourea to lead was just slightly less than 1:1. These ratios help to

confirm the following equation for the overall reaction which had previously been postulated by several workers:

$$Pb^{++} + (NH_2)_2\,CS + 2OH^- = PbS\downarrow + H_2NCN + 2H_2O.$$

It was found that the reaction was initially slow, increased to a relatively constant rate, and then tapered off. It is believed that the induction period (i.e., the slow initial rate) was indicative of autocatalysis by the PbS formed during the reaction. The induction period could be completely removed by the addition of powdered PbS, and the initial reaction rate was approximately proportional to the amount of PbS added. Attempts were made to determine the reaction orders with respect to the biplumbite ion (the predominate lead-bearing ion), the hydroxide ion, and thiourea. They varied with time, indicating the complex nature of the reaction. The reaction rate was increased by the addition of small amounts of dust or powdered PbS; it was decreased by stirring (this hastened the coagulation of the autocatalyst, PbS), by the addition of small amounts of polyvinyl alcohol or cupric salts, and by using solutions of sodium hydroxide that had been aged in glass containers. Experimental evidence was obtained to demonstrate that the reaction did not involve the formation of sulfide ions by the alkaline hydrolysis of thiourea, followed by the precipitation of lead sulfide. It is believed that one of the steps of the reaction is the formation of a lead-hydroxide-thiourea complex, which subsequently decomposes to lead sulfide.

FILM STUDIES

As part of the Laboratory's continuing investigation of the mechanism of photoconductivity, a series of measurements on seven Eastman Kodak, lead sulfide, chemically deposited films have been used as the principal tools for this study. On the basis of these measurements, several interesting phenomena have been observed. First, the lifetime in these films appears to be controlled by the Fermi level. The apparent density of empty traps is the same in all films. In order to account for the dependence of the lifetime on temperature, one must use cross-sections which vary exponentially with reciprocal temperature. The mobility in all these films is remarkably similar and independent of light bias.

An automatic field effect apparatus has been developed to speed up measurements. A program of study of lead selenide films has also been undertaken. Evaporated film studies will also begin shortly in an attempt to identify the precise impurities responsible for the field effect and photoconductivity.

LEAD TELLURIDE CRYSTAL PREPARATION

A technique for pulling PbTe crystals has been developed and it has been described in earlier reports. During the past year the effort in this program has been directed toward growing oriented single crystals and n-type single crystals. There are two reasons for growing oriented single crystals (1) to study the effect of orientation on the growth process and (2) to produce oriented single crystals for specific experiments. The PbTe phase diagram is such that crystals grown from melts prepared from stoichiometric proportions of Pb and Te are always Te rich and therefore p-type. For this reason the crystals prepared in the initial phases of this program were all p-type. A number of experiments have been carried out on these p-type crystals. It would be desirable to carry out these and other experiments on n-type crystals produced by the same technique.

Since the technique of pulling crystals from the melt always makes use of a seed, only minor modifications of the technique are necessary in order to grow oriented crystals. The seed holder has been redesigned to hold oriented single crystals which have been cut and ground to shape from pulled crystals. Equipment has been purchased and installed which will greatly facilitate the cutting out of oriented seed crystals. The only other problem is the starting of crystal growth such that the new crystal takes on the orientation of the seed. This is accomplished by initially melting away the worked surfaces of the seed, then proceeding with the growth in the normal manner. These alterations in the growth technique and the installation of a better temperature controller have not only produced large oriented single crystals, but have resulted in an increase in the overall reliability of the process. At present only growth in the $\langle 100 \rangle$ direction has been attempted giving crystals like the one shown in Fig. 2. Other high symmetry directions will be attempted in the near future. Preliminary experiments indicate that these oriented crystals will make possible very accurate measurements of the elastic constants and of the internal friction in PbTe.

From a practical point of view, the attempt to produce n-type single crystals has not yet succeeded. The first method tried consisted of growing or attempting to grow crystals from melts containing various amounts of excess Pb in order to produce crystals which contained excess Pb and would therefore be n-type. Although these experiments failed to produce good n-type crystals, they did give information about the phase diagram of PbTe near its maximum melting point. For example, they indicated that solid PbTe with stoichiometric proportions is in equilibrium with a melt which contains more than 6 Pb atoms for each 5 Te atoms. With the present technique of crystal growth, inclusion of a second phase

Fig. 2. Photograph of single crystal of lead telluride grown from the melt. The crystal has <001> orientation, as can be seen from the 90° angle between the faces. Magnification 3 X.

consisting of almost pure Pb occurs with melt compositions less Pb rich than those necessary to produce a stoichiometric crystal. These results are consistent with the PbTe phase diagram which has been determined at this Laboratory. Preliminary doping experiments with Bi and I indicate that these two impurities behave in a similar manner; that is large amounts of impurities must be added to the melt in order to incorporate small amounts into the crystal.

AN ASPECT OF THE PHASE DIAGRAM OF LEAD TELLURIDE

The compound semiconductor lead telluride is stable over a narrow range of composition. The deviations from stoichiometry act like impurities in elemental semiconductors. At present deviation from stoichiometry is important in determining the carrier concentration in undoped lead telluride. Gibbs' phase rule implies that when one fixes the temperature of the crystal all the intensive variables of the three-phase (liquid, solid and vapor), two-component system are fixed. Previous work at this Laboratory has determined the temperature-composition projection of the three-phase line. This project is concerned with a determination of the temperature-pressure projection of the three-phase line. The results of these two experiments will completely determine the three-phase line. This will lead to a more complete understanding of the properties of the compound, and will allow crystals to be prepared with more accurately controlled characteristics.

The pressure-temperature projection is determined in the following manner: A crystal is placed in one end of a silica tube and pure tellurium is placed in the other. The system is then evacuated and sealed off. The tube is placed in a furnace which is so constructed as to allow separate control of the temperature of the tellurium, which determines the tellurium vapor pressure in the furnace, and of the crystal temperature. (see Fig. 3) One then fixes the temperature of the tellurium and varies the crystal temperature, or vice versa, until the crystal just begins to melt. The vapor pressure of the tellurium and the temperature of the crystal at which melting just occurs determine one point on the temperature-pressure projection of the three phase line.

PRECIPITATION OF Pb and Te in PbTe CRYSTALS

The rate of precipitation of Te in PbTe single crystals has been studied at temperatures in the range from 180°C to 400°C. In p-type crystals the thermoelectric power was used to monitor the changes, since at

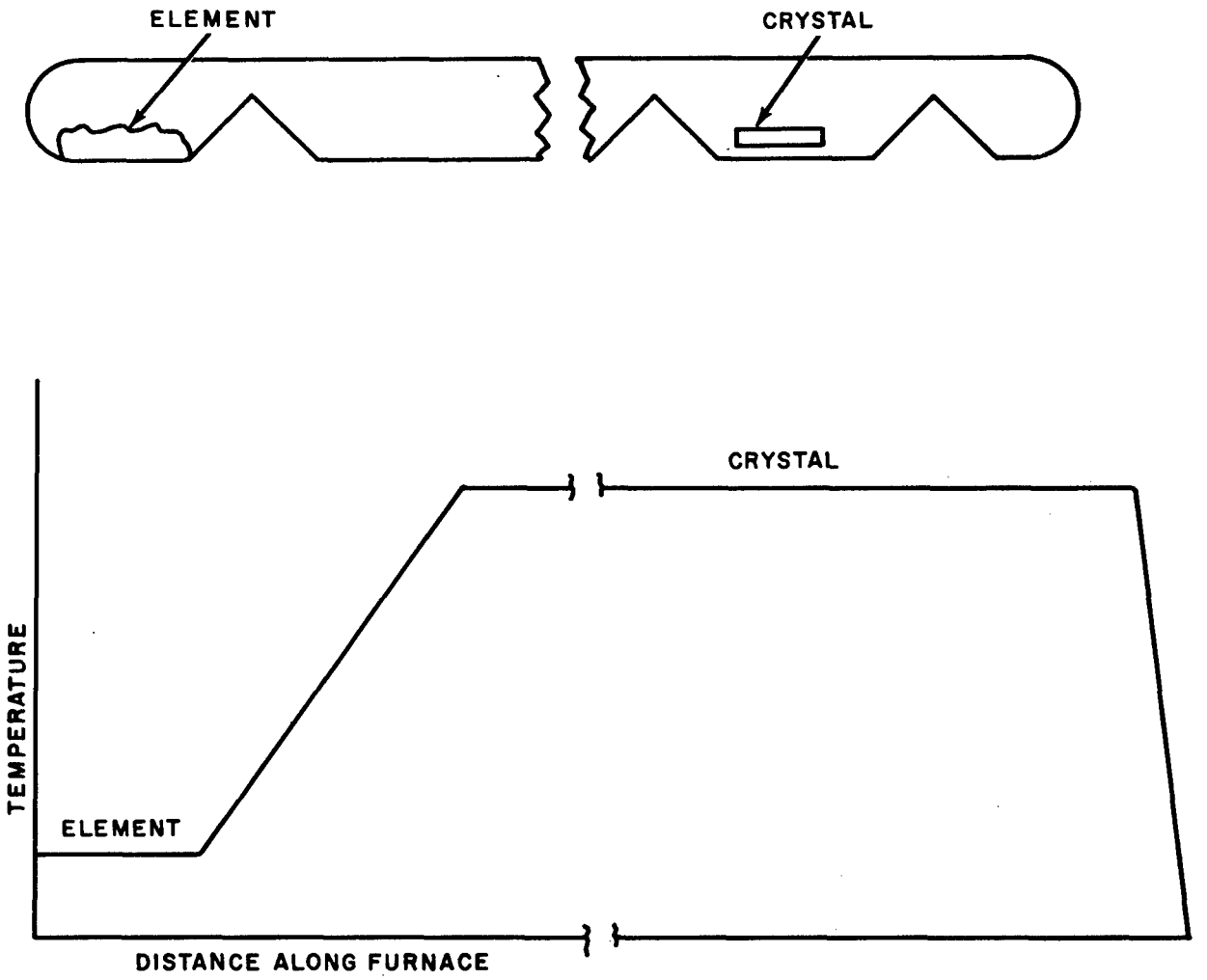

Fig. 3. Schematic representation of temperature along the furnace used in the study of the three phase line.

the temperatures involved, the thermoelectric power is a very sensitive indicator of the composition change resulting from internal precipitation.

In n-type crystals all the electrical properties are in the intrinsic range at the annealing temperatures of interest so that samples had to be cooled to room temperature periodically to evaluate the composition changes which had taken place. The results of these studies on precipitation phenomena in PbTe provide experimental data to be compared with existing theories of precipitation in solids. The experimental data of composition versus a reduced time parameter shown in Fig. 4 is in good agreement with the rate given by a stress assisted precipitation theory of Ham, where precipitation takes place on dislocations. The radius of the precipitation centers calculated from the experimental data is in reasonable agreement with the one given by the theory.

The second purpose of these studies was to provide a simple method for obtaining crystals of n and p-type PbTe having specific values of carrier concentration approaching the stoichiometric composition.

The curve of Fig. 5 shows carrier concentration as a function of annealing temperature obtained from these studies. The equilibrium time for the various temperatures is given in Fig. 6 for crystals having about 10^5 dislocations/cm^2. Rates would be less for a higher dislocation concentration.

Data on precipitation rates in n-type crystals have not been as complete yet, but the data show the same general behavior observed in p-type crystals. The rate of reaching equilibrium is slower in n-type crystals than in p-type crystals corresponding to a slower diffusion rate for Pb than for Te in PbTe crystals. This supports the vacancy model for n-type PbTe over the interstitial model. While equilibrium has not been reached as yet in current studies on n-type PbTe at 240°C, carrier concentrations have been reduced from about an initial value of 1×10^{18} to $9 \times 10^{16}/cm^3$. Further studies will be made in order to find the equilibrium value at this temperature and compare the rate with the theory. PbTe crystals having carrier concentrations considerably less than $9 \times 10^{16}/cm^3$ will be obtained from these experiments.

THERMOELECTRIC POWER IN p-TYPE PbTe CRYSTALS

There is considerable effort reported in the literature on thermoelectric power in high carrier concentration PbTe. However, there is little on low carrier density material. Since the precipitation technique

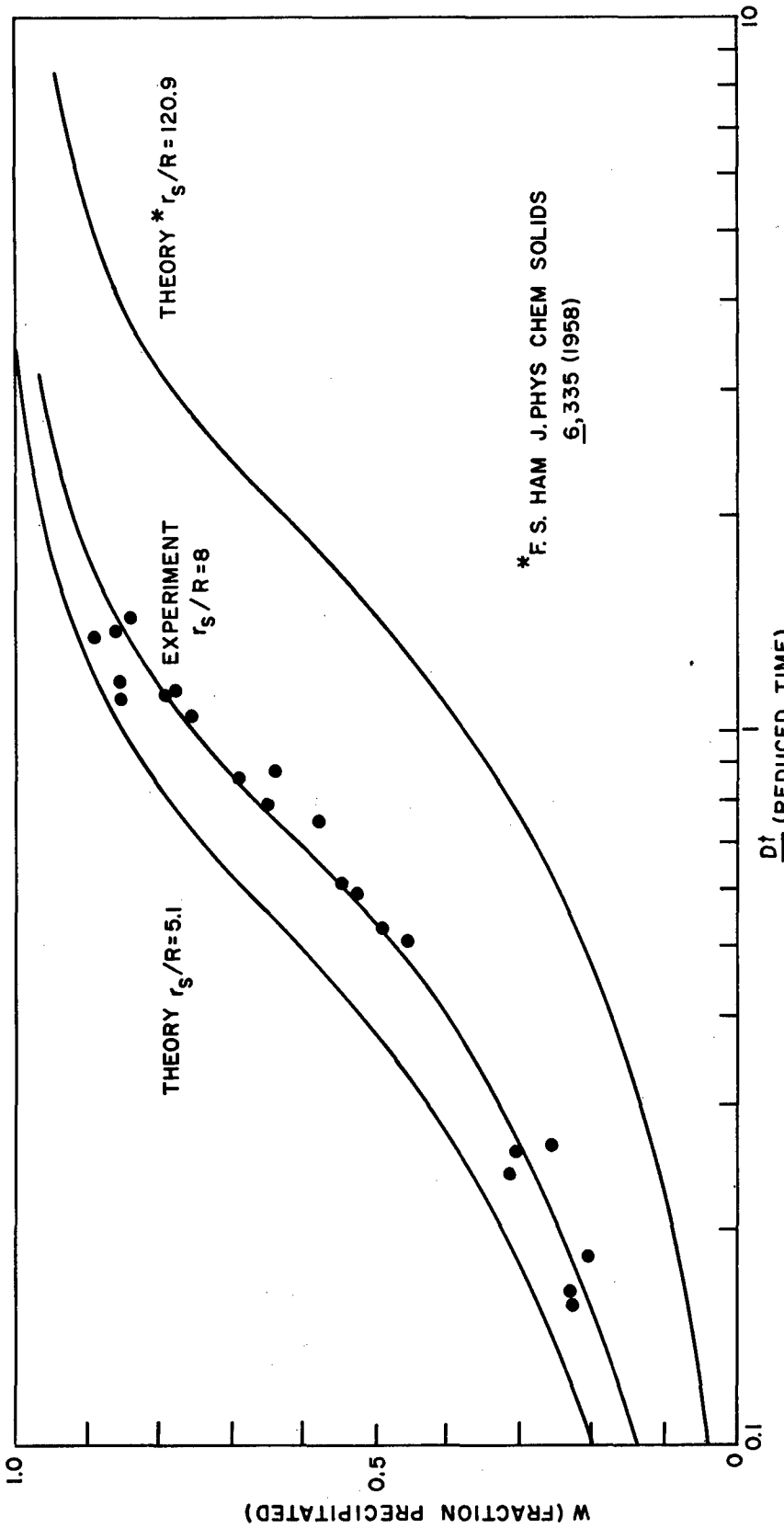

Fig. 4. Precipitation rate of Te in PbTe crystals.

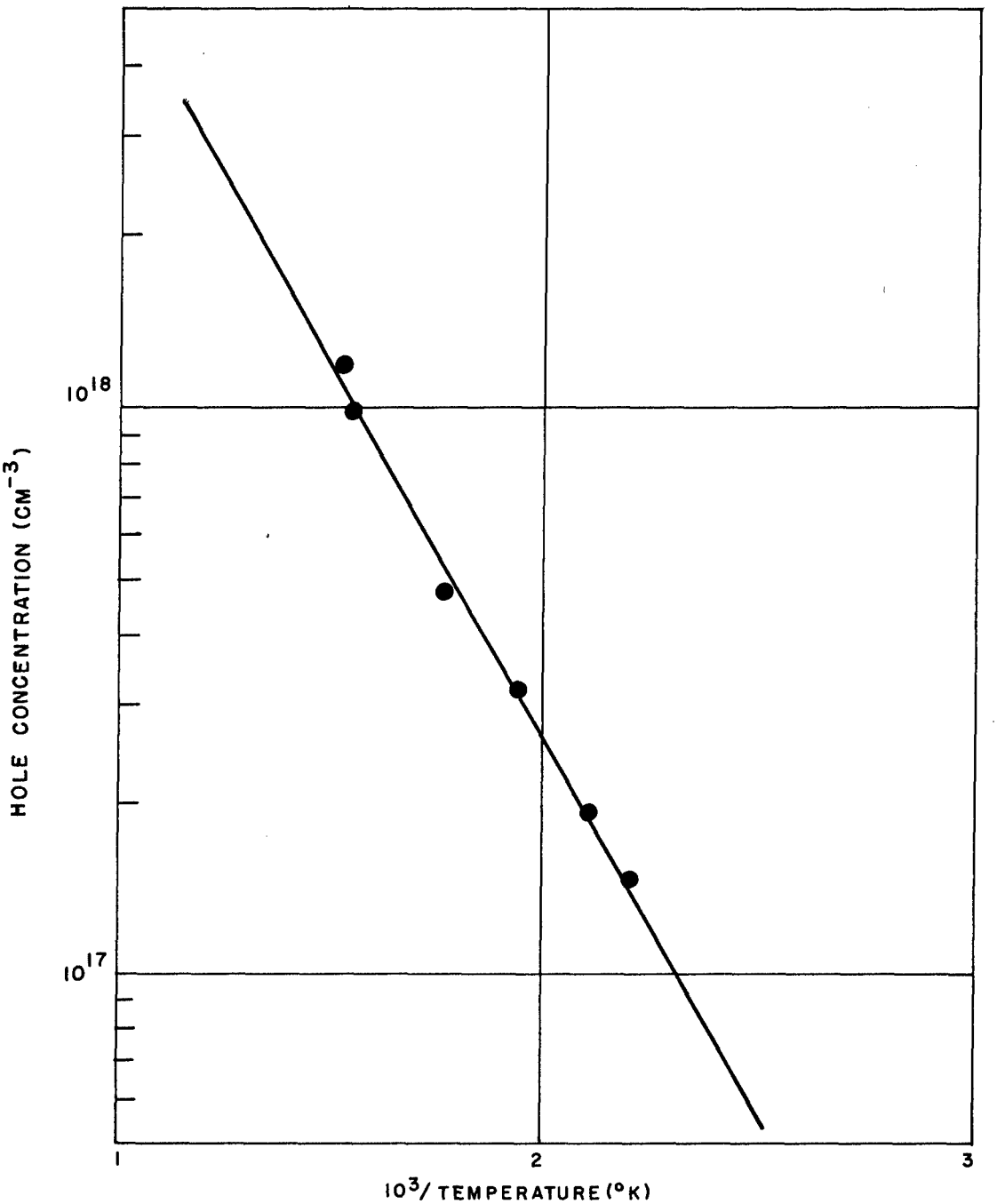

Fig. 5. Precipitation of Te in PbTe crystals.

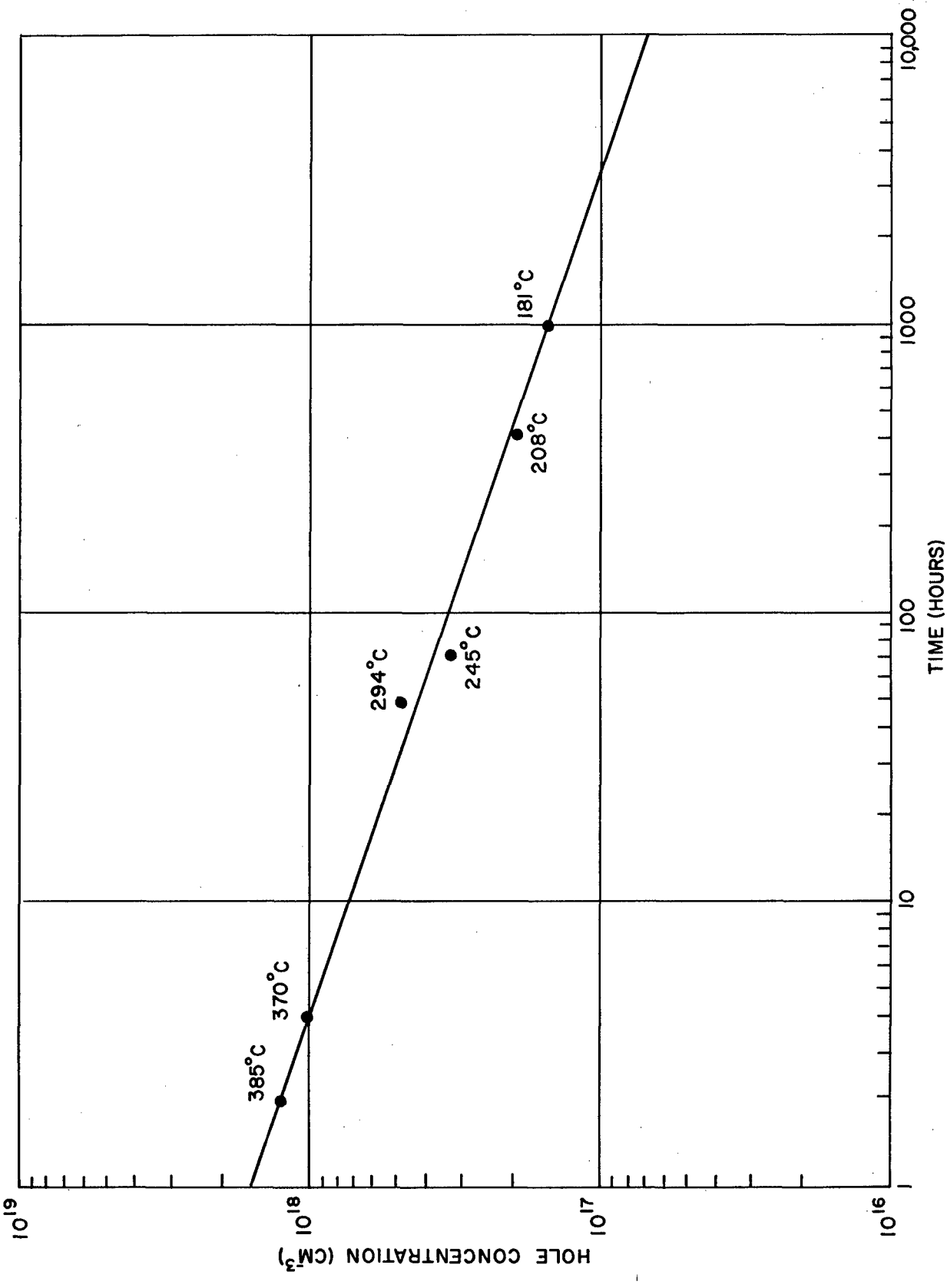

Fig. 6. Precipitation of Te in PbTe.

produces crystals having a range of carrier concentration down to near intrinsic values it is appropriate to study the thermoelectric properties of such crystals.

Thermoelectric data were taken in the temperature range from liquid nitrogen to 400°C or less depending upon the crystals. The results are shown in Fig. 7. Data on the room temperature values of carrier concentration, resistivity and mobility are shown in Table I.

TABLE I

p-TYPE PbTe CRYSTALS

p (cm^{-3})	ρ (ohm-cm)	μ (cm^2/volt sec)
3.1×10^{18}	.0023	870
1.0×10^{18}	.0091	680
4.8×10^{17}	.0189	690
3.3×10^{17}	.026	730
1.9×10^{17}	.041	790
1.5×10^{17}	.058	715

PHONON DRAG EFFECTS IN PbTe

Phonon drag effects in semiconductors appear as an additional contribution to the thermal emf, generally at low temperatures where phonon and electron wavelengths become comparable in length. By reducing the carrier concentration sufficiently in PbTe crystals through the precipitation process it has been possible to observe the effects of phonon drag at temperatures at and below liquid nitrogen temperature. The curve of thermoelectric effect in Fig. 8 shows the increased thermal emf at temperatures below -195°C which is characteristic of phonon drag.

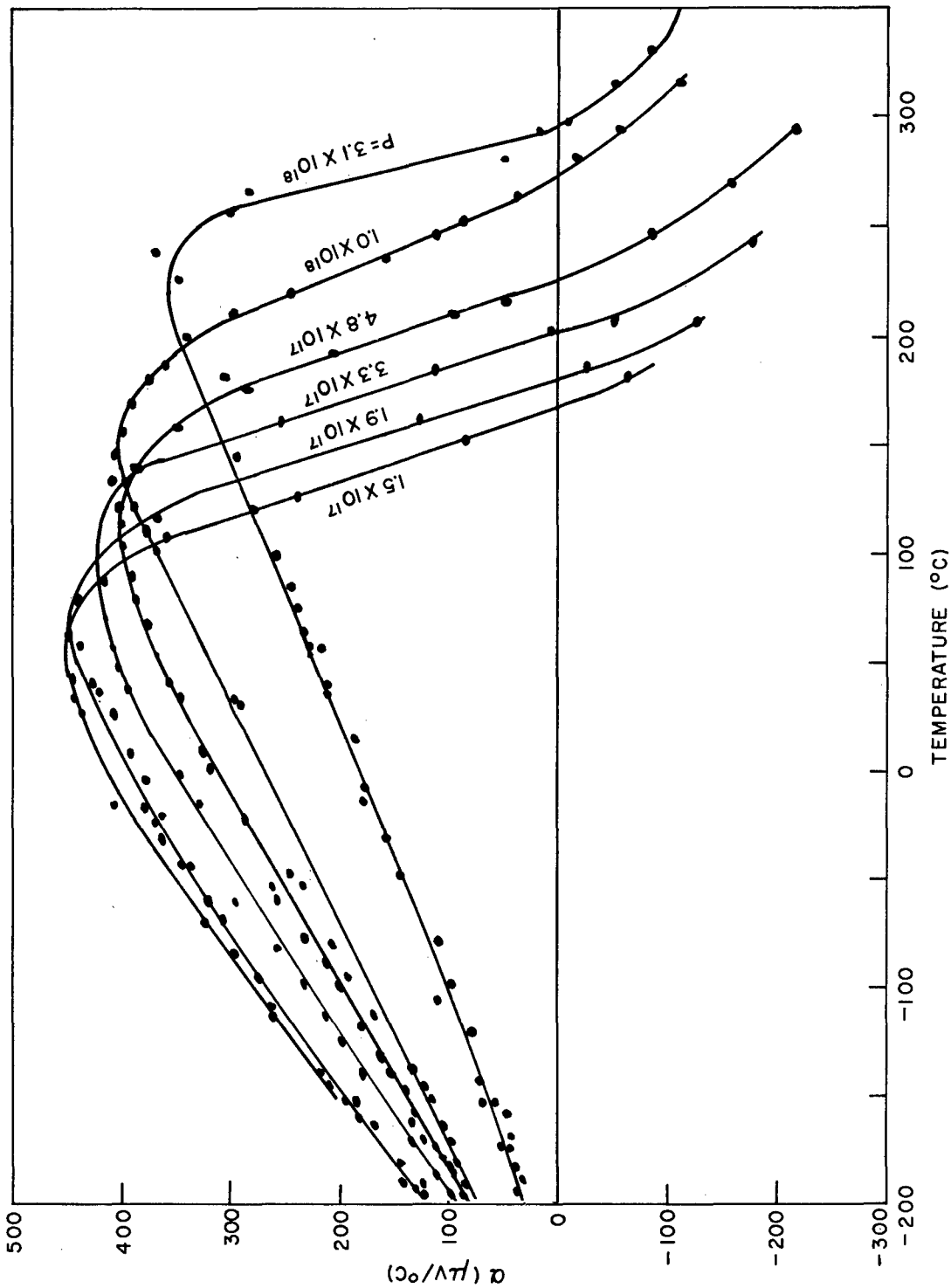

Fig. 7. Seebeck Effect in P-Type PbTe

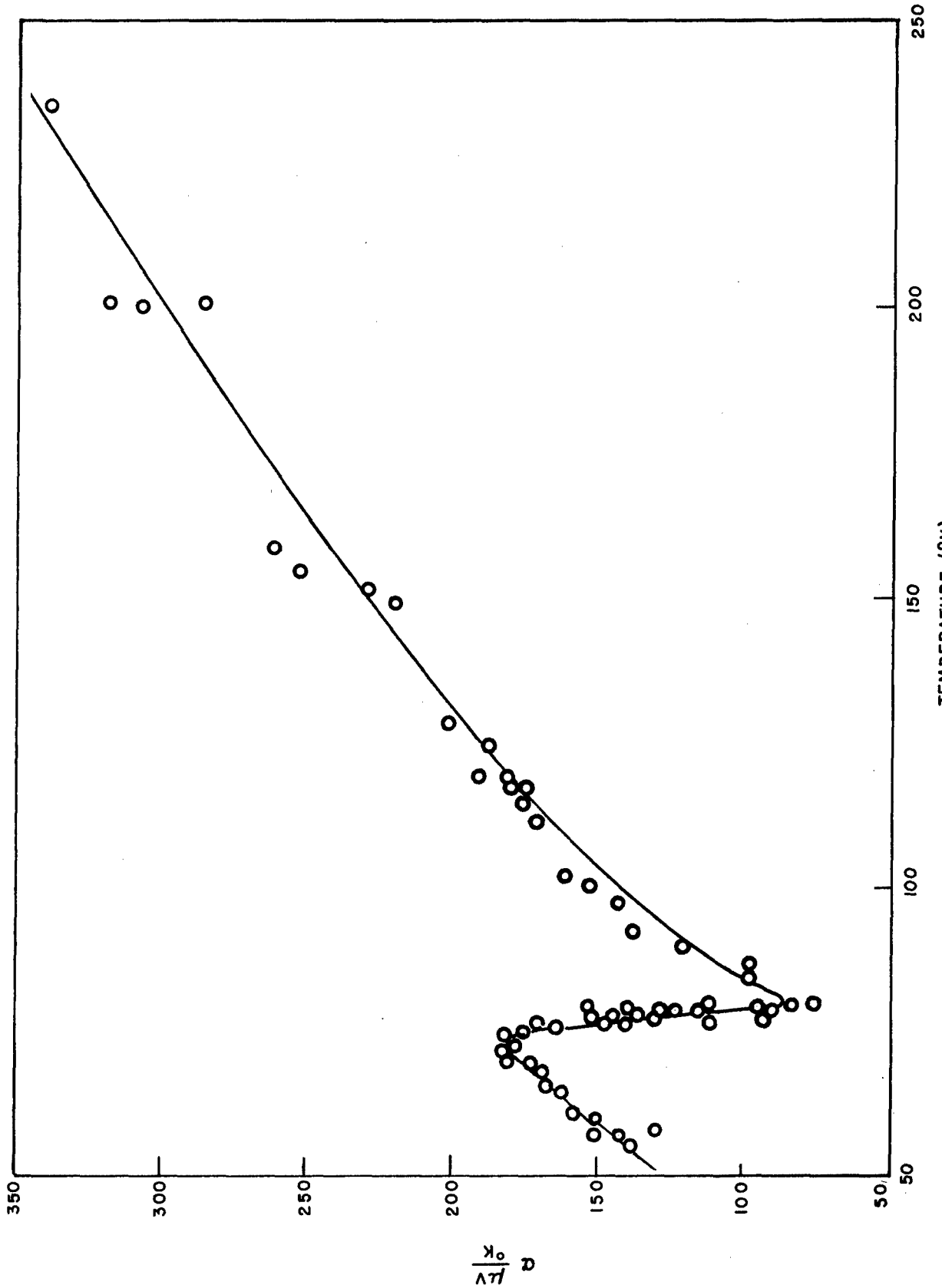

Fig. 8. Seebeck Effect in P-Type PbTe p = 1.5 x $10^{17}/cm^3$

COMPOSITION STABILITY LIMITS OF PbTe

Previously we have described experiments in which single crystal PbTe was made as Pb-rich or Te-rich as possible at a given temperature. It was then quenched and its room temperature carrier concentration was determined. The resulting curves of carrier concentration versus anneal temperature are of great importance both from a practical and fundamental point of view. The relatively large scatter of the data from Pb-rich, n-type, PbTe indicates that possibly foreign impurities and/or quenching effects were significant. As a result the experiments are being repeated using purer PbTe crystals (pulled from the melt), fused silica, carbon-coated fused silica, and spectroscopically pure graphite crucibles, and a variety of quenching rates.

Thus far, it has been found that for Pb-rich PbTe (1) the scatter of data is considerably reduced, (2) the crystals are less n-type than found previously, having 3.5×10^{17} carriers per cm^{+3} after annealing at 600°C, instead of 1.5×10^{18} cm^{-3}, and (3) the crystals are relatively stable at room temperature in contrast to previous results. Preliminary indications are that our earlier results were significantly affected by the presence of bismuth at a concentration of about 10^{18} atoms/cm^3. Further investigation of impurity effects on the properties of the lead salt semiconductors is under way.

THEORY OF STABILITY LIMITS OF SEMICONDUCTOR COMPOUNDS

The theory of the defect solid state has been useful in relating the chemical composition and electrical properties of semiconductor compounds. Although it is recognized that every crystalline compound is stable over some range of composition, the question as to the magnitude of this range has not previously been answered. Such a range of stability in general implies a corresponding range in electronic carrier concentrations and since it is difficult experimentally to distinguish between the existence of a small range of compositions and the presence of foreign impurities, theoretical guides are useful. Therefore, the problem has been approached using the general features of the accepted model of non-metallic crystals. In particular, the statistical mechanical analysis of this model serves to furnish expressions for the chemical potentials of the crystal components which are the heart of the solution.

Two types of atomic point defects (vacancies or interstitials) are assumed to be predominant in the crystal and furnish a mechanism by which

the crystal can exist over a range of composition. The atomic point defects are randomly distributed in the crystal and their creation requires a constant expenditure of energy so long as their concentrations are small. Clustering is neglected. A single donor level is assumed to be associated with each defect of one type, and a single acceptor level with each defect of the other type. For non-degenerate semiconductors of this type an analytical solution can be obtained for the limits of stability of the compound for cases in which the phases coexisting with the compound at its limits of stability are the pure elements. It is found that the limits of stability at any temperature are further apart (1) the more negative the free energy of formation of the semiconductor compound and (2) the smaller the ratio of the square of the intrinsic carrier concentration to the product of the concentrations of the two types of atomic point defects in the ionized state. On the other hand, the limits of stability are shifted to metal-rich, n-type compositions (1) the larger the difference in the free energies per mole of the pure elements (both measured relative to infinitely dispersed atoms in their lowest quantum states) and (2) the more negative the difference between the energy required to create the atomic point defect associated with the donor level (that predominates in metal-rich material) and the energy required to create the atomic point defect associated with the acceptor level.

SURFACE TRANSPORT

The major new experimental and theoretical work at NOL in the field of surface transport has been the study of the surface-dependence of the thermoelectric power. The experimental results indicate that in thin high resistivity germanium samples, the total thermoelectric power of the specimen is a sensitive function of the excess surface charge in the space charge region. The theory for this process has been developed, and detailed computations are in progress.

The overall agreement between theory and experiment is remarkable, as can be seen in Fig. 9. However, the theory does not distinguish between diffuse or specular surface scattering of the excess carriers. Two promising areas of study here are the effect of surface scattering of phonons on phonon drag in the space charge region and the effect of high surface fields on the effective mass of the excess carriers. Both of these studies will entail measurements at lower temperatures. Since partially specular scattering has been observed by others at these lower temperatures this is a region of great interest.

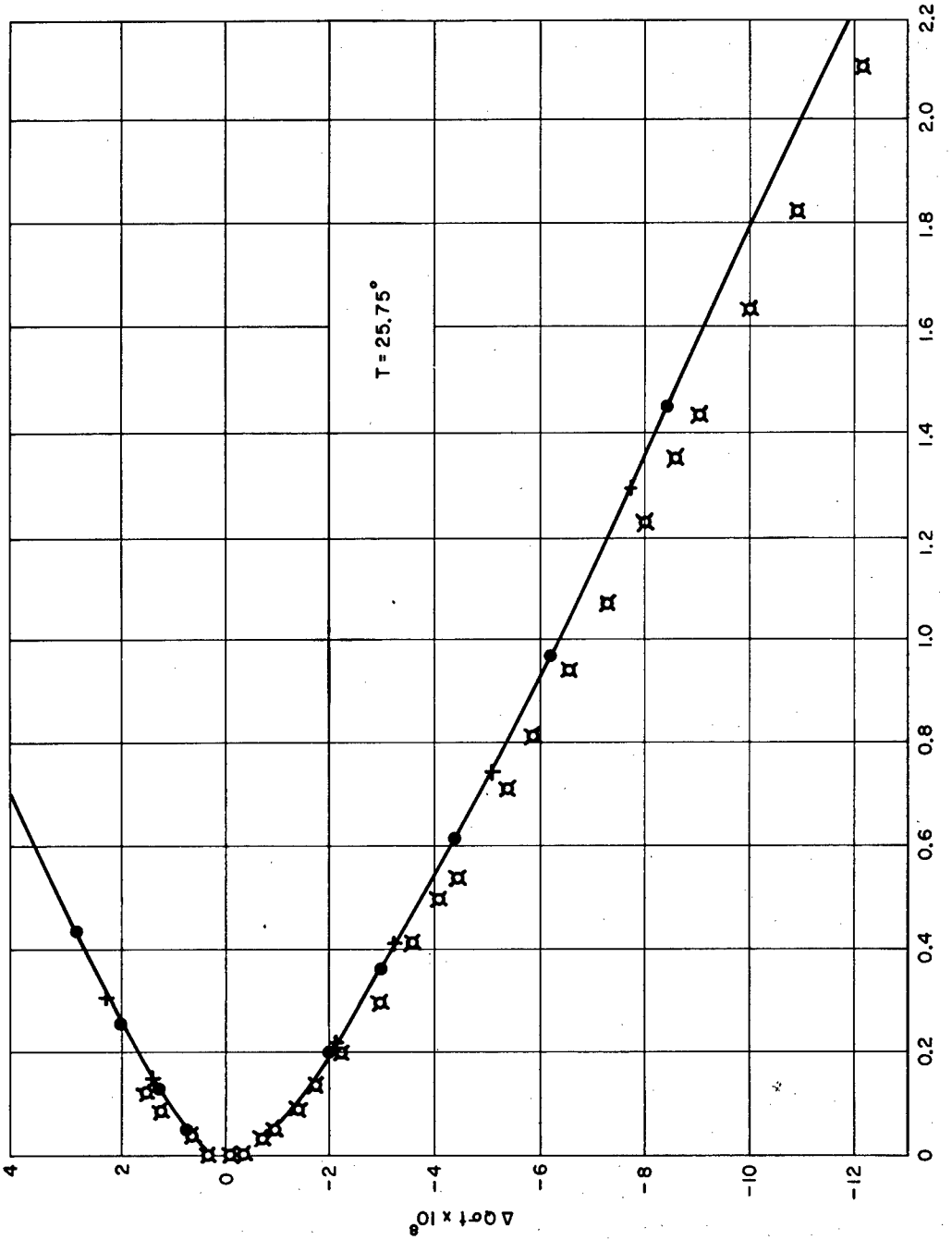

Fig. 9. Change in the sheet electrical conductance times the thermoelectric power as a function of the fractional change in conductance of the sample with respect to the conductance minimum. ⌘ are experimental data, + are calculated points assuming specular scattering and ● are calculated points assuming diffuse surface scattering.

RECOMBINATION LIFETIME

In any semiconductor device the average time taken for an electron to combine with a hole is one of the critical parameters. We are investigating physical mechanisms governing this lifetime in the intermetallic semiconductor indium antimonide by measuring the lifetime at low temperatures in InSb prepared under different conditions and with varying carrier concentrations. Because of the very short lifetimes in indium antimonide, they are best deduced from measurements of the photoconductivity and the photoelectromagnetic effect. Photoconductivity measurements determine the change in conductivity of a sample produced by photoexcited electrons and holes. In the photoelectromagnetic experiment these electrons and holes diffuse away from the surface in a magnetic field. The paths of the carriers are bent by the field, producing a voltage across the sample which is measured as in a Hall effect experiment.

The uniformity of samples has been checked by illuminating small areas of the sample and measuring the photoconductivity of these areas. The results of these measurements indicate that our best samples are uniform to 10%. Surface recombination has proven a more difficult problem. To measure the effect of surface recombination, the samples were illuminated with light of varying wavelength which penetrates the sample to varying depths, thus allowing the relative effects of surface and bulk recombination to be measured. It is found that the surface is rather important in controlling the magnitude of the photoeffects, and that it tends to fluctuate with time. Several surface treatments mentioned in the literature were tried in an attempt to find one that would reduce surface recombination to insignificance. None of these gave results which were satisfactory. Use of a low pressure nitrogen discharge induced by a Tesla coil has helped to reduce the surface recombination. Measurements of lifetime on various samples of InSb are now underway.

MAGNETOMETERS

There is considerable current interest in the development of a high accuracy sensitive magnetometer for antisubmarine warfare purposes. Recently several new kinds of quantum mechanical magnetometers have been developed that seem to be quite promising. To a large extent their properties and limitations have not yet been fully established.

We have undertaken an examination of the spectra of various atomic gases to determine whether substances other than those already used might provide possibilities for improved magnetometers. To be useful

the substance must have a long lived state which exhibits Zeeman splitting and a suitably spaced non-branching pump state of proper angular momentum.

NEW FLUX-GATE MAGNETOMETERS FOR USE WITH SINGLE STRIP PERMEAMETERS

Two new sensitive flux-gate magnetometers of the second harmonic type have been developed for use as H-measuring systems of a d-c single-strip permeameter. Both are employed with a simple bridge circuit which eliminates the necessity of complex filters and selective amplifiers and allows operation over a wide range of frequencies independent of source frequency stability. The first magnetometer is an open-magnetic-circuit type of two Supermalloy cores. The second magnetometer is a closed-magnetic-circuit type which does not influence the field being measured. The magnetometers were designed to measure fields from 1 milli-oersted to about 10 oersteds, although these are not physical limits of sensitivity.

MAGNETIC MOMENT MEASUREMENT

The measurement of magnetic moments of materials containing transition metal atoms gives information on the number of electron spins per atom or molecule as well as a measure of the internal fields in the sample. For materials that are ferro- or ferrimagnetic the magnetic moment becomes saturated and as the magnitude of the magnetic field is increased a few thousand gauss no increase in magnetic moment is observed. In materials that are paramagnetic or antiferromagnetic, and in ferro- or ferrimagnetic substances above their Curie points, the magnetic moment is more or less proportional to the magnetic field and this proportionality constant is called the susceptibility. In some cases the susceptibility is slightly field dependent such as in antiferromagnetics and in materials containing ferromagnetic impurities. From susceptibility measurements we can study antiferromagnetic interactions and obtain additional information on the effective magnetic moment of each atom as well as a measure of the exchange fields between atoms. Studies have been made on a chromium metal single crystal which is antiferromagnetic and on the effect of lithium substitution in manganese ferrite, a ferrimagnetic material.

The magnetic susceptibility of a chromium single crystal was found to be almost constant at approximately $3.25 \pm .05 \times 10^{-6}$ emu/gm over the temperature range 673°K to 77°K. The sample was in the shape of a cylinder (weight .3058 gms); measurements have been made along both a

[100] and [111] direction, but no anisotropy effects were observed. At 4.2°K the susceptibility increased to 4.00×10^{-6} for the [111] direction and 3.90×10^{-6} in the [100] direction. This crystal was part of the same specimen used by Corliss, Hastings and Weiss in their neutron diffraction investigation in which they observed a Néel or Curie temperature of 308°K. From neutron diffraction measurements another magnetic anomaly has been reported at 158°K by Bykov and co-workers in the U.S.S.R. and also by Hastings at the Brookhaven National Laboratory. The measurements reported here indicate that corresponding changes in the susceptibility are less than 0.5×10^{-6} emu/gm. The data are illustrated in Fig. 10.

When lithium, which is monovalent, is substituted in a ferrite, there is a rearrangement of valances. For manganese ferrite we obtain $Mn^{++}_{1-2x}\ Li^{+}_{x}\ Mn^{++}_{x}Fe_2^{+++}O_4^{--}$. Thus, for each lithium atom added one manganese atom goes from divalent to trivalent. Samples were prepared with x = 0.1, 0.2, 0.3, 0.4 and 0.5. Fig. 11 is preliminary data, because we do not know the quality of the samples. An interesting point is the rise in Curie temperature as lithium is added; it is very rare to find a non-magnetic atom substitution which raises the Curie temperature.

The magnetic moment per molecule drops with lithium content at a rate suggesting that the lithium is going to the B sites. For compositions x = 0.3, 0.4 and 0.5 the moment is somewhat lower than can be accounted for on this scheme without a more drastic rearrangement of the ions.

RARE EARTH MAGNETIC ALLOYS

The work on rare earth alloys has centered mainly about the compounds GdX_5 where X is Fe, Co, Mn and Cu or combination of two of these. From the work on substitutions in these compounds it has been possible to show that the moments of the Co atoms in the compound $GdCo_5$ are antiparallel to those of the Gd atoms while the moments in the compound $GdFe_5$ are arranged Gd↑ 2 Fe↑ 3 Fe↓. From this result it was apparent that the saturation magnetization of the $GdFe_5$ compound could be increased by substituting a light atom or an atom having a smaller moment for an iron atom having an anti-parallel orientation (B site). This was accomplished by substituting a Co atom for an iron atom but when two Co atoms were substituted the second atom replaced one of the Fe atoms having a parallel orientation (A site) and the moment was again reduced. An attempt was made to substitute a boron atom for an Fe atom in a "B" site but the boron atom substituted into an "A" site with a resulting decrease in the moment of 2.22 μ_B. When a Mn atom was substituted for an Fe atom the Mn atom

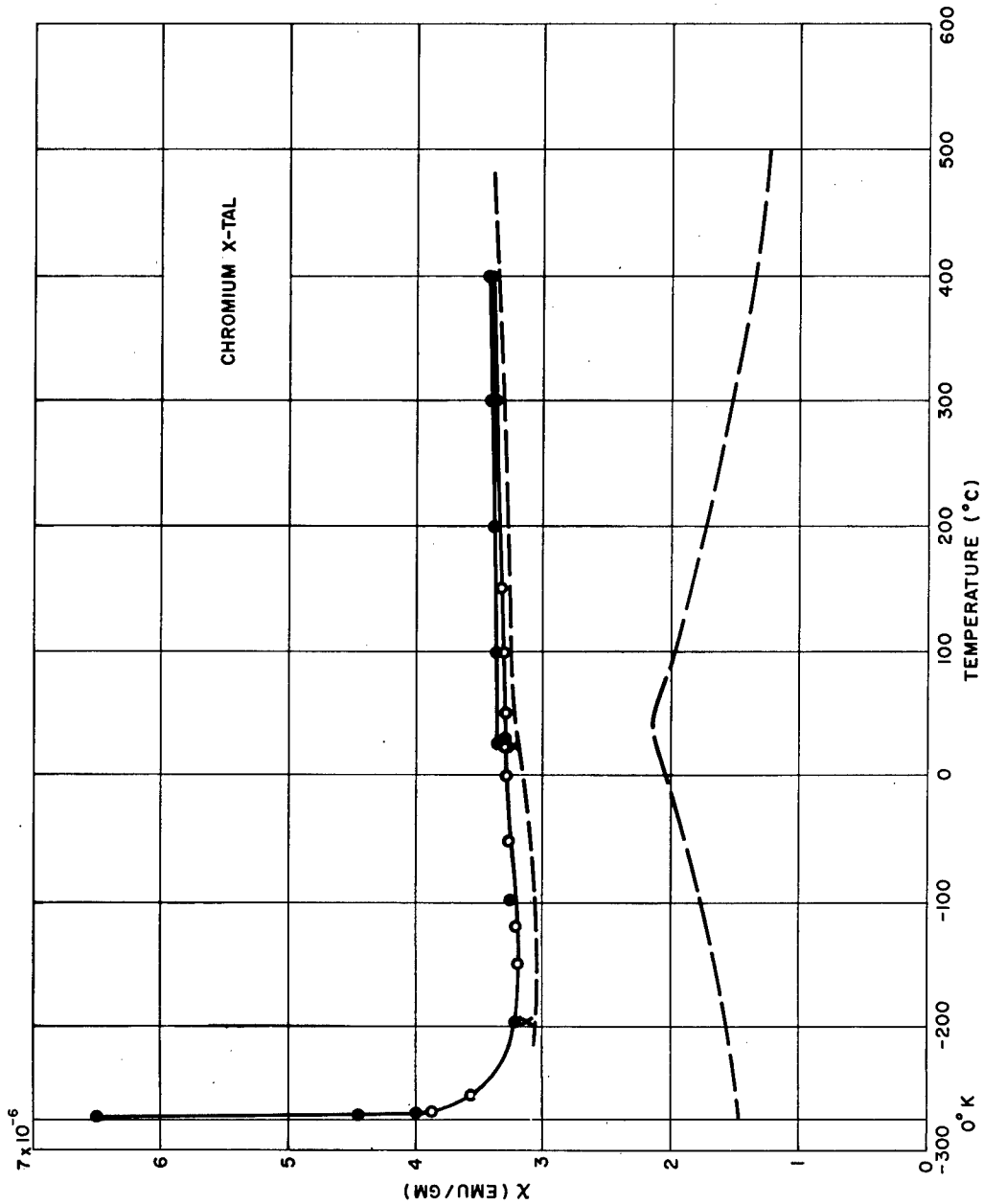

Fig. 10. Magnetic susceptibility as a function of temperature for a chromium single crystal. Open circles are for the magnetic field H along a [100] direction. Closed circles are for H along a [111] direction. The crosses are data points taken when the sample was cooled in a field of 10,000 gauss along [100] from 70°C to -196°C. The higher dashed curve is the data of Lingelback (Z. Physik. Chem. 14, 1 (1958)). The lower dashed curve is calculated for antiferromagnetic behavior assuming 0.4μ_B per atom and a θ value of -310°K using the Curie-Weiss law, $\chi = C/(T + 310)$.

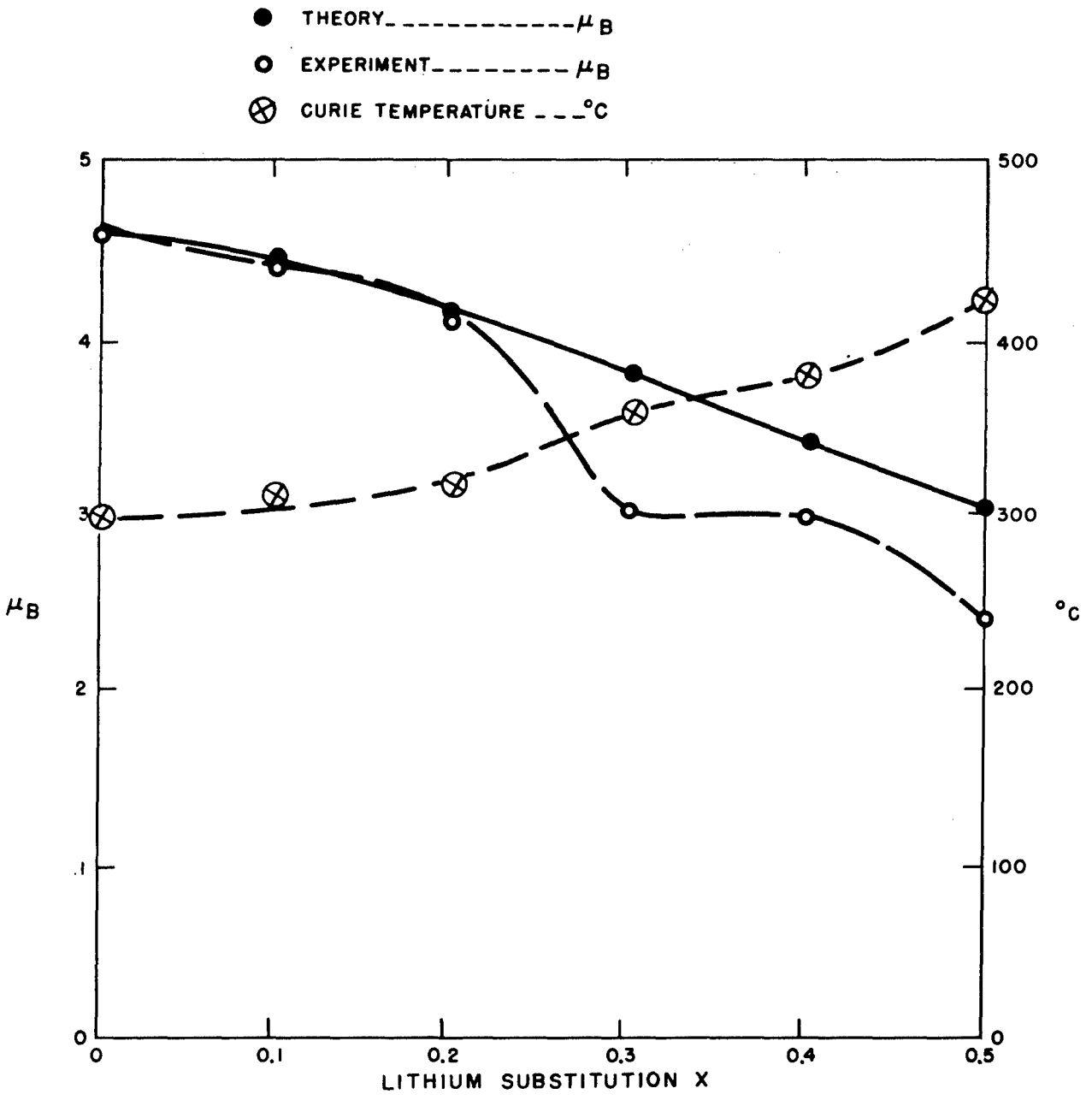

Fig. 11. Magnetic moment estimated at 0°K and Curie temperature for $Mn_{1-x}Li_xFe_2O_4$. The theoretical curve is calculated on the basis that all the lithium goes into the B sites.

substituted into a "B" site with an apparent moment of 5 μ_B which reduced the moment of the compound by ~2.8 μ_B.

CATION ORDERING IN $Mn_xFe_{3-x}O_4$

It has been reported that there is a pronounced minimum in the first anisotropy constant of the spinel $Mn_xFe_{3-x}O_4$ at about x = 0.7. Reasonable assignment of cations to A and B sites suggests that near this composition, about half the A sites are populated with Mn^{2+} ions, and that A site ordering may accompany this minimum. This conjecture has been tentatively confirmed by neutron diffraction, as discussed elsewhere in this report.

It is of interest to consider the possible arrangements of sublattice spin directions in the spinel as a function of composition. We have generalized the Yafet-Kittel model slightly to allow for umbrella arrangements. Such a model is capable of yielding the observed moment dependence. An investigation of the validity of this picture is in progress.

IMPROVED SONAR TRANSDUCER MATERIALS

At the request of BuShips and Naval Electronics Laboratory, San Diego, California, NOL has developed a magnetic core material with an overall improvement of 29% magnetic characteristics for a high power, broad band, variable reluctance sonic transducer. The core material should have a high flux density at low bias magnetizing forces with a high incremental permeability and a low incremental core loss. At present the theoretical efficiency of the variable reluctance transducer is about 80%. Since the size of the power plant for the range and frequencies involved is quite large, any increase in the efficiency of the transducer would permit a more compact design or increase its output.

The improvement was accomplished by developing a technique to cut a strain sensitive, domain-oriented 49 Co, 49 Fe, 2V magnetic core material known as Supermendur. Up to this time it had been considered impossible to retain the excellent toroidal magnetic characteristics after bonding and cutting by usual commercial techniques. The method developed at NOL consists of rigid encapsulation of the Supermendur core in an aluminum box and cutting it by electrolytic erosion. The resulting degraded cut surfaces were then carefully lapped until no further improvement of its magnetic characteristics occur. The magnetic evaluation of this cut core showed a 43% greater residual induction and a 15% greater maximum induction than the presently used silicon-iron core material. The

results are now being evaluated by NEL for possible adoption of the improved core material in the variable reluctance transducer design.

SOFT MAGNETIC ENVIRONMENTAL ALLOYS

The rapid advancements in military and space technology have placed increased environmental demands on magnetic and electronic control devices and components. These demands have necessitated evaluation of existing magnetic alloys and development of new and improved systems that would be resistant to adverse environmental effects caused by elevated temperatures, nuclear radiation, shock, vibration and acceleration.

The relative stability of the iron-silicon alloys (from 0 to 6.5% silicon) in ambient temperatures up to 500°C was thoroughly studied. It was found that the isotropic alloys showed more stability than the high purity, specially oriented alloys. These alloys were also quite stable in nuclear radiation environments having a total integrated neutron flux of approximately 2×10^{18} nvt.

The iron-silicon alloys were also found to be quite responsive to magnetic annealing cycles, particularly those alloys containing from 4% to 6.5% silicon (by weight). An increase in maximum permeability values from 17,000 to 70,000 has resulted from exposure of a 5% silicon-iron alloy to a magnetic annealing cycle. NavWeps Report 7331 summarizes the intrinsic advantages of the iron-silicon system over other existing soft magnetic alloy systems for these various environments previously stated.

Investigation of magnetic alloys in the iron-aluminum system was started during the past year. Alloys containing aluminum weight percentages from 0 to 10% are being studied since the 10% - 16% area has been thoroughly covered in previous reports.

The major advantage of the iron-aluminum system over the iron-silicon system has been that of improved ductility. Alloys containing up to 5% aluminum have been reduced to thin tapes having as much as 99.5% cold reduction without causing undue strain on processing equipment. There have been no magnetic advantages observed for the iron-aluminum system over the iron-silicon system thus far; however, this investigation is still in progress.

RADIATION DAMAGE THRESHOLDS FOR PERMANENT MAGNETS

Alnicos, Cr Steel, and Cunico irradiated to 5×10^{20} epicadmium neutrons/cm^2 at 55°C showed only slight changes in magnetic open circuit induction. Barium ferrites, Co Steel, and Silmanal showed major changes, while the change in Cunife was intermediate. These results are due to irradiation alone, since 55°C is sufficiently close to room temperature so that temperature effects are absent. It is to be noted that of the two most commonly used magnetic materials, the Alnico family is very resistant to neutron irradiation, while the barium ferrite family is least resistant.

Previous NOL work showed that all important permanent magnet materials can withstand 10^{17} epicad n/cm^2 at 90°C without significant change in magnetic properties. Hence the radiation damage threshold (10% change in magnetic properties) lies above 10^{17} for all permanent magnets and above 10^{20} for Alnico II, V, XII, 3-1/2 Cr Steel and Cunico I at normal temperatures.

TABLE II

RADIATION EFFECTS ON PERMANENT MAGNETS
5×10^{20} epicad n/cm^2 at 55°C

Material	% Change in Open Circuit Induction	
Alnico II	-2.5	
Alnico V	-2.5	
Alnico XII	-6.5	Small Changes
3-1/2 Cr Steel	+2.5	
Cunico I	-7.5	
Cunife I	+13.	Intermediate
36 Co Steel	-37.	
Silmanal	-46.5	
Barium Ferrite I	-50.5	Major Changes
Barium Ferrite V	-63	

In a combined radiation - high temperature environment of 5×10^{20} epicad n/cm^2 at temperatures up to 325°C, the Alnicos changed less than 5%, and

Cunico I around 10%. All others changed in excess of 20%, decreases in open circuit induction ranging from 23 to 97%.

The above results are the first data reported on magnetic changes in permanent magnets produced by neutron irradiation. They have immediate application in the design of electromagnetic flowmeters for AEC and military reactor development.

MAGNETIC ANISOTROPY

In addition to the isotropic exchange energy, due to the interaction between the spins of a magnetic system, there is a magnetic free energy term which depends upon the orientation of the spins with respect to the crystal axes. One must do work with an external magnetic field to rotate the magnetization from an easy to a hard direction. This work is the anisotropy energy.

This anisotropy energy in turn reacts back upon the magnetization. When the anisotropy energy is small compared to the exchange, perturbation methods are applicable. We have derived perturbation expansions which show that in this case the magnitude of the magnetization depends upon its direction; the magnetization is larger in easy directions than in hard ones at any particular temperature. However, perturbation methods lead to a Curie temperature which is independent of direction.

In materials of low exchange energy and large anisotropy different methods of analysis must be employed. We have analyzed the problem of a spin one internal field Hamiltonian with a one-ion uniaxial anisotropy term. In this case it results that, in addition to the previous effect, the Curie temperature also depends upon the direction of the magnetization. Fig. 12 shows the dependence of the Curie temperature, which is proportional to $1/a_c$ (kT_c/exchange energy), on the direction of the magnetization. θ is the angle between the magnetization and the crystal $\underline{c}$ axis. This is depicted for a number of values of the parameter λ, which is the ratio of the 0°K anisotropy energy to the exchange energy.

LONGITUDINAL FERRIMAGNETIC RESONANCE

In previous work, the magnetic resonance properties of three-sublattice ferrimagnetic systems were calculated and it was shown that a new effect should exist for systems with triangular configurations. For the usual arrangement of external magnetic fields in which the constant field

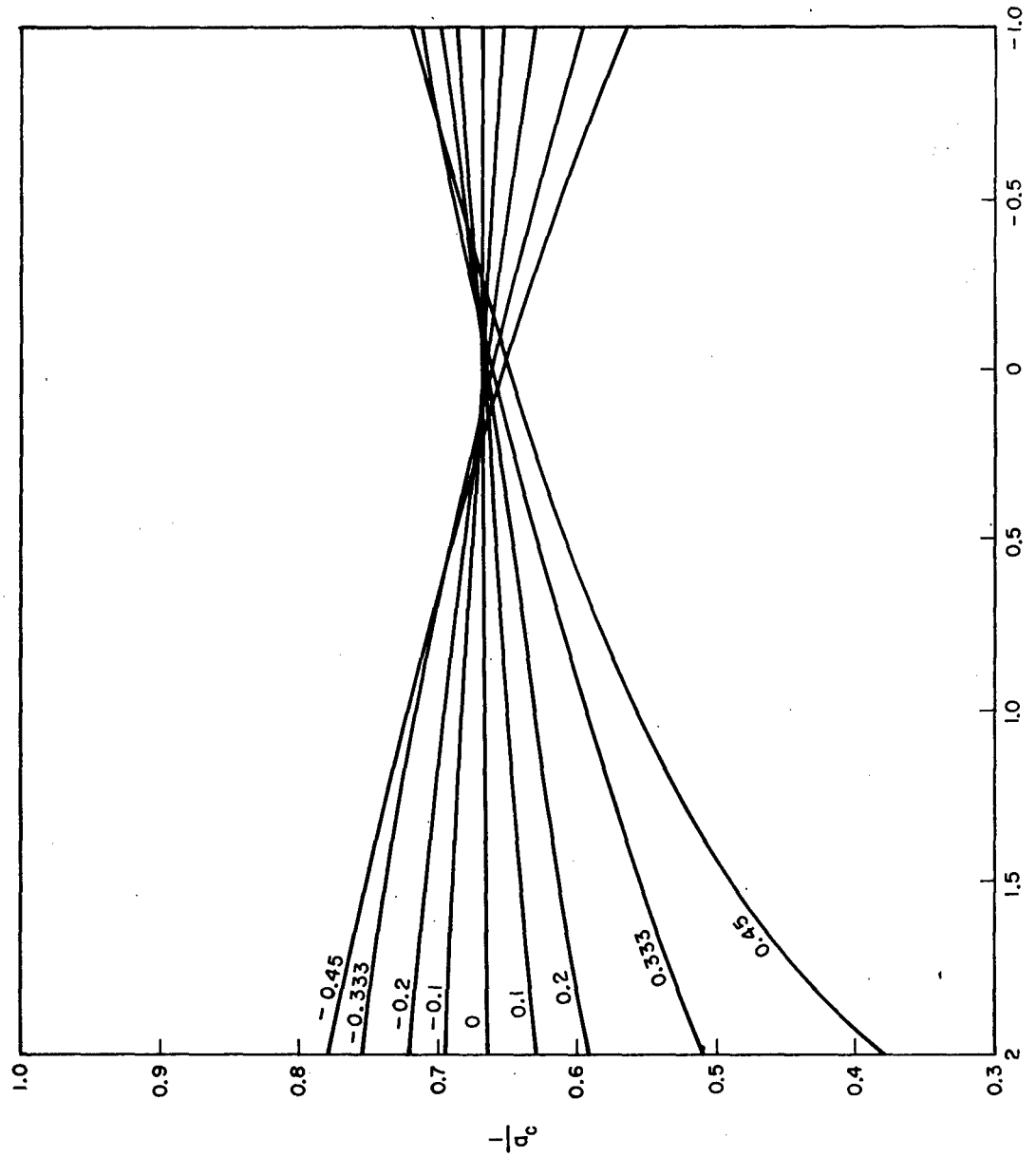

Fig. 12. The dependence of the Curie temperature on the direction of the magnetization for various values of the parameter λ.

is parallel to the net magnetization and a small oscillating field is perpendicular to this direction, this effect consists in the production of an oscillating magnetization component which is parallel to the net magnetization (and hence perpendicular to the oscillating field). This magnetization component has the same frequency as the applied field and does not arise from the non-linear terms in the equations of motion. The origin of this effect can be qualitatively understood by referring to Fig. 13. The general effect of the oscillating field is to set the sublattice magnetizations into precession about their static orientations. As shown, the precession of sublattices 2 and 3 will give rise to this new oscillating component along the direction of the net magnetization in addition to the transverse x and y components.

If one studies this figure further, we see that the situation depicted then suggests the possibility of two more new effects associated with triangular configurations if the oscillating field is now applied parallel to the common direction of the constant field and the net magnetization rather than perpendicular to it. The first of these effects consists in the production of an oscillating component in the transverse x-y plane by the extreme field which is in the z-direction of the net magnetization. The second effect involves the simultaneous occurrence of an oscillating magnetization component parallel to the oscillating field. The relevant susceptibility components were calculated for this case to see if these effects, which were suggested by the above qualitative arguments, were actually quantitative consequences of the equations of motion. It was found, in fact, that these effects should exist in principle, and they now await experimental confirmation.

TABLES OF PROPERTIES OF FERRITES

Magnetic ferrites have been worked with for some thirty years. During the last decade many studies have been published as represented by a thousand or more scientific papers. Because the scattered location and variable quality of these papers make it difficult to locate the most reliable data, the Physical Properties of Materials Division has maintained on a limited basis a file of various magnetic properties.

We have been invited to contribute similar information, but in a more detailed and expanded form, to the Landolt-Bornstein Tables. The Landolt-Bornstein volumes are a valuable and authoritative source concerning the physical properties of materials. A volume on magnetic substances is now in preparation. Our contribution as submitted is about 100 pages devoted to nickel ferrite and its substitutional derivatives, ferrous ferrite,

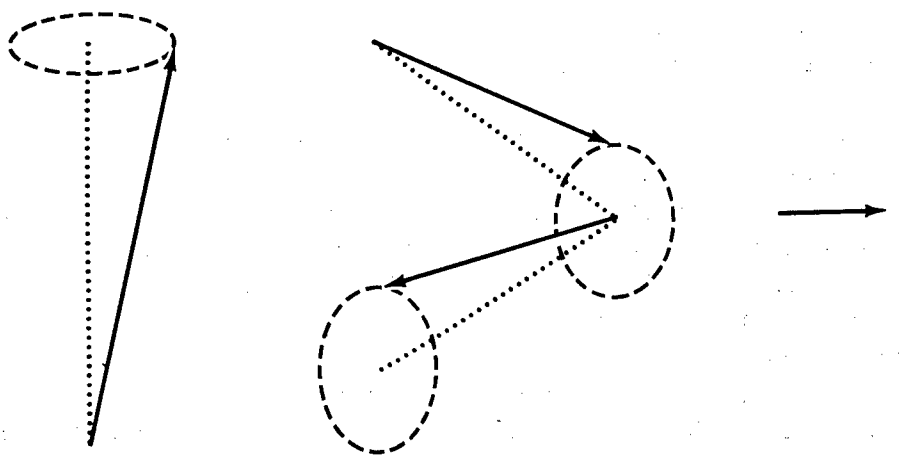

Fig. 13. Origin of the oscillating magnetization component which is transverse to the exciting field.

and various chromites. It represents, however, only a small part of the volume, which when published, should be a valuable reference work for all investigation in the field of magnetism.

MICROWAVE AMPLIFIERS

Under a microwave amplifier project supported by the BuWeps, advances have been made in both the theory of microwave amplification and in the testing of materials and components. The materials and components portion of the project is reported here.

Initial exploratory experiments ranged from optical resonance effects coupling effects within the skin depth of ferromagnetic metals, to phases discrimination effects. The latter yielded a down converter to 30 Mc/sec with gain and a phase discriminatory structure employing 10 Kmc/sec pump or power frequency and 5 Kmc/sec signal frequency which had modest gain More conventional cavity structures with semiconductor diodes as the active elements were constructed. These rectangular and cylindrical cavities were operated in the degenerate mode with both Microwave Associates' Pill Varactor diodes and Texas Instruments' GaAs diodes. Negative results were obtained due to a combination of things such as improper impedance matching and load termination. To investigate the non-degenerate cavity diode amplifier, a structure employing two coupled rectangular cavities was constructed and tested; then two coaxial amplifiers modeled after the Harris amplifier were constructed and tested. Fig. 14(a) shows these three amplifiers. The larger coaxial cavity amplifier was designed for 870 mc/sec signal frequency using approximately 10 kilomegacycles/sec pump frequency. It was operated as an upper-sideband upconverter, a lower-sideband upconverter and a negative resistance amplifier. The smaller coaxial cavity amplifier was designed for signals in the C band range (3.95 - 5.85 kilomegacycles/sec) and employed approximately 10 kilomegacycles/sec pump frequency. Fig. 14(b) shows this amplifier with tuners attached and the parts identified. Both of these amplifiers employed Microwave Associates' MA 450H Varactor Diodes. In midyear the decision was made to build a magnetic microwave amplifier using single-crystal Yttrium Iron Garnet. Sphere grinders were constructed and grinding and polishing techniques developed with the objective of producing a highly polished sphere of single crystal YIG having a resonance line width of approximately 1/3 oersted. Imperfections in the surface of the sphere generate spin waves which broaden the intrinsic line width. A ferromagnetic resonance spectrometer was designed and assembled to monitor the line widths as the polishing proceeded. This instrument employs a swept magnetic field and crystal detection, the resultant resonance curve

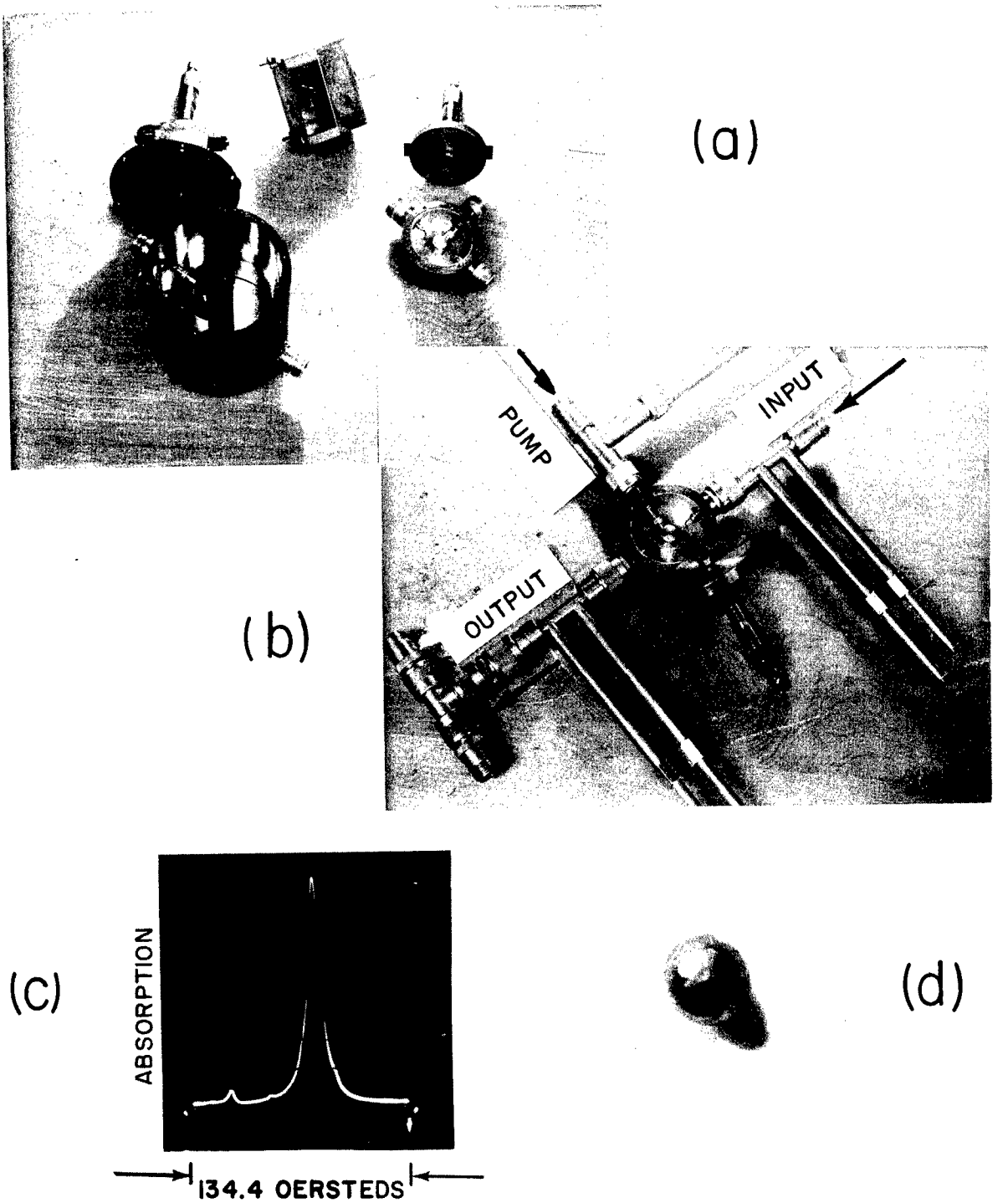

Fig. 14. Microwave Amplifiers and Elemental Components
(a) Cavity Type Microwave Amplifiers Using Semiconductor Diodes
(b) Cavity Type Amplifier with Stub Tuners
(c) Ferromagnetic Resonance in YIG Sphere
(d) YIG Sphere with Polished Surface

being displayed on an oscilloscope. The sample sphere is placed in a position of maximum magnetic field, and minimum electric field in a rectangular waveguide cavity operating in the TE_{103} mode. Fig. 14(c) shows a resonance curve for a polished sphere at a frequency of 5.14 kilomegacycles/sec. The large absorption is the principal precessional mode while the smaller absorptions are due to magnetostatic modes of higher wave number. Fig. 14(d) shows the polished surface presently being obtained on single crystal YIG spheres. The sphere diameter is 0.030 inches. To date the minimum line widths obtained are approximately 4 oersteds. Although highly polished over most of the area the samples exhibit what apparently is porosity in certain areas.

An analysis of the dispersion spectrum of ferromagnetic permeability and its relation to coaxial line measurements has been made. The spectrum can be approximately represented in terms of μ_o, the d.c. initial permeability, and b, the magnetic viscosity coefficient. Included are the effects of magnetic viscosity on coaxial line measurements of the complex permeability spectrum. Inclusion of this effect enables one to calculate the error involved in using the standard conversion formulas between displacement minimum and standing wave ratio of coaxial line measurements and the real and imaginary parts of the complex permeability, respectively. Data have been obtained which indicate the existence of errors between the measured permeabilities given by the standard conversion formulas and the true complex permeability.

SINGLE CRYSTAL NEUTRON DIFFRACTION STUDIES

The single crystal studies of the past year have been concerned not so much with determination of magnetic structures as with measurement of the form factor, or the variation of magnetic cross section with angle. This quantity is the Fourier transform of the scattering density, and so provides information about the d-electron charge distribution. Two cases of interest have been investigated, one of metallic binding (the alloy Fe_3Al) and the other of ionic binding (NiO). The measurements on Fe_3Al, which is ferromagnetic, were made by using a polarized neutron beam. NiO, which is antiferromagnetic but does not have a unique spin axis, is unsuitable for this technique and a non-polarized neutron beam was used.

In both these cases the form factors were measured out to high scattering angles ($\sin \theta/\lambda \sim 0.8 - 0.9$) and showed characteristics of an aspherical charge density. They have been analyzed by comparison with theoretical form factors calculated by Weiss and Freeman from free-atom Hartree-Fock wave functions, taking into account crystalline field effects.

As expected from crystal field theory, the unpaired spin density of Ni^{2+} was found to have e_g symmetry, with lobes pointing along cubic [100] directions. The Fe_3Al required some admixture of t_{2g} states, in which the spin density is peaked along the body diagonal. The departure from spherical symmetry is perhaps less understandable for the latter case, since crystalline field effects in metals are expected to be small. The Fe_3Al data have been used to obtain a two-dimensional projection of the unpaired spin density by Fourier synthesis.

POWDER NEUTRON DIFFRACTION STUDIES

During the past year the neutron diffraction experiments carried out previously by our Laboratory personnel at the Naval Research Laboratory have been relocated and combined with our effort at the Brookhaven National Laboratory. The kind of information that is best determined by these experiments, namely, spin alignment and cation positions, is illustrated by the powder diffraction studies that have been made during this period.

The problem involving cation positions was an Fe-rich manganese ferrite, in which a one-to-one ordering of the Mn and Fe on the tetrahedral spinel sites had been hypothesized; this ordering proved to be detectable because of the fact, peculiar to neutron diffraction, that these two cations have scattering amplitudes of opposite sign. A low temperature investigation of the spin alignment of two rhombohedral carbonates, $MnCO_3$ and $FeCO_3$, was aimed at relating the symmetry of the antiferromagnetic structure to the weak ferromagnetism observed in the former compound. A slight canting of the spins, which had been proposed as the origin of this moment, is compatible with symmetry if the spins are perpendicular to the trigonal axis, and incompatible if they are parallel; the spin axes determined by neutron diffraction are as predicted if this mechanism is correct.

INTERMETALLIC COMPOUND MATERIALS FOR HIGH TEMPERATURE APPLICATIONS

Intermetallic compounds, in general, are characterized by brittleness, hardness, abrasion resistance, high electrical resistance and complex atomic arrangements. Similar to ceramics and cermets, many intermetallic compounds have some advantageous mechanical and physical properties but suffer mainly from a lack of ductility at ambient temperatures. Since many of the intermetallics have high melting temperatures, it was decided

to reexamine the potential of this class of materials for structural high temperature applications. Considerable effort was first devoted to the selection of a series of intermetallic compounds or compound-base alloys and then to study them in more detail for suitability in structural application.

The initial detailed effort was concerned with the compounds of titanium and nickel from 33 to 75 w/o Ni. Included in this range are the three identifiable compounds Ti_2Ni, TiNi, and $TiNi_3$. Of the three, the equiatomic compound TiNi appears most interesting. This compound is unique in that it is not brittle at ambient temperatures. Table III shows some of the physical and mechanical properties obtained in this Laboratory on a stoichiometric TiNi alloy containing 55.1 w/o Ni. Coupled with the desirable ductility of TiNi is its ability to be deformed and fabricated both hot and at room temperature.

Some prior investigators who studied the phase equilibria of the Ti-Ni alloy system found the low temperature stability (below about 830°C) of the TiNi phase in doubt, claiming that it dissociated into the two adjacent compound phases of Ti_2Ni and $TiNi_3$. Many of these investigators employed X-ray diffractometer scans of stress-relieved TiNi filings as a medium for their phase equilibria studies. Present study yielded similar results when employing TiNi filings. X-ray diffractometer studies performed on annealed arc-cast alloys from 50 to 60 w/o Ni revealed a different result. Those alloys below 52 w/o Ni decomposed into Ti_2Ni and $TiNi_3$ at lower temperatures. The Ni-Ti alloys containing more than 52 w/o Ni exhibited a sizeable amount of TiNi phase at room temperature with small percentages of Ti_2Ni and $TiNi_3$ coexisting. As the Ni content increased beyond about 57 w/o Ni the amount of TiNi phase lessened and the $TiNi_3$ phase increased gradually in accordance with a second version of the constitution diagram. A plot of the quantity of coexisting phases as a function of w/o Ni and its relationship to the two versions of the TiNi constitution diagram is given in Fig. 15.

Hot hardness data on the three compounds Ti_2Ni, TiNi, and $TiNi_3$ are shown graphically in Fig. 16. Two curves are given for TiNi since the compound is body centered cubic when randomly oriented and a CsCl type structure when ordered. The major difference in the two TiNi curves shown in Fig. 16 is the "secondary hardening" peak exhibited by the disordered material. This phenomenon could be related to lattice imperfections and their distribution induced by rapid cooling or it may be a result of minor quantities of a second phase, i.e., Ti_2Ni or $TiNi_3$ present with the TiNi phase. The production of a phase-pure TiNi material and the determination of its hot hardness properties should yield a better understanding of the mechanism.

TABLE III

SOME PROPERTIES OF THE TiNi PHASE (55.1 w/o Ni-Ti)

PHYSICAL

Density (25°C), gr/cm^3	6.45
Melting Point, °C	1240 - 1310
Melting Point, °F	2264 - 2390
Crystal Structure	CsCl (B.C.C.)
Lattice Parameter, Å	3.015
Electrical Resistivity (25°C), microhm-cm	~80
Electrical Resistivity (900°C), microhm-cm	~132
Linear Coef. of Expansion (24 - 900°C), per °C	10.4 x 10^{-6}
Recrystallization Temperature, °C	550 - 650

MECHANICAL

Tensile

Ultimate Tensile Strength, psi	125,000
Yield Strength, psi	81,400
Young's Modulus, psi	11.2 x 10^6
Tensile Elongation, %	8.1

Transverse-Bend

Modulus of Rupture, psi	216,000
Modulus of Elasticity, psi	11.3 x 10^6
Impact Strength (0.297 in^2 bar), ft-lbs	24
Hardness, R_C	29 - 34

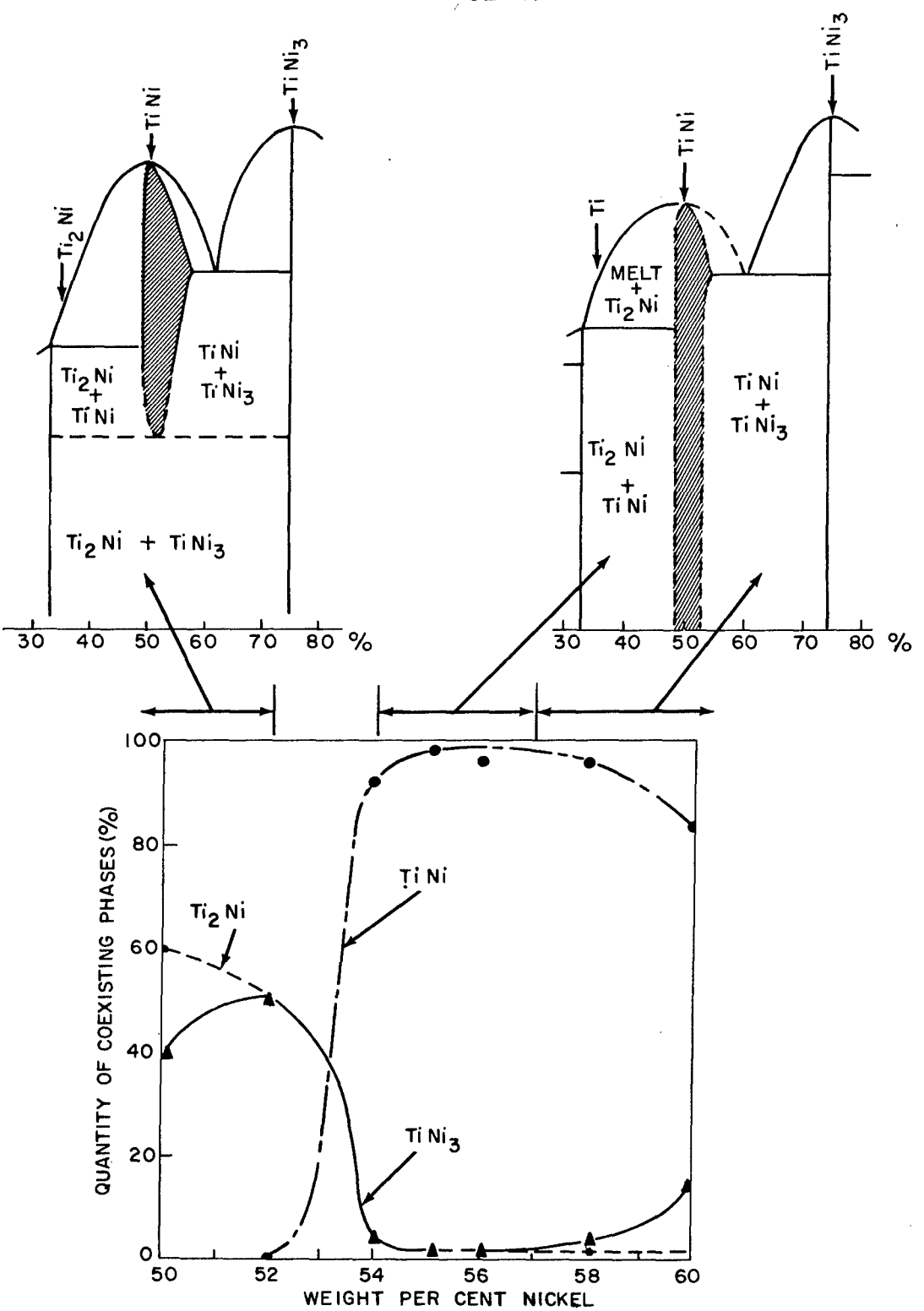

Fig. 15. Room Temperature Phase Relationship of Nickel-Titanium Alloys from 50 to 60 w/o Ni

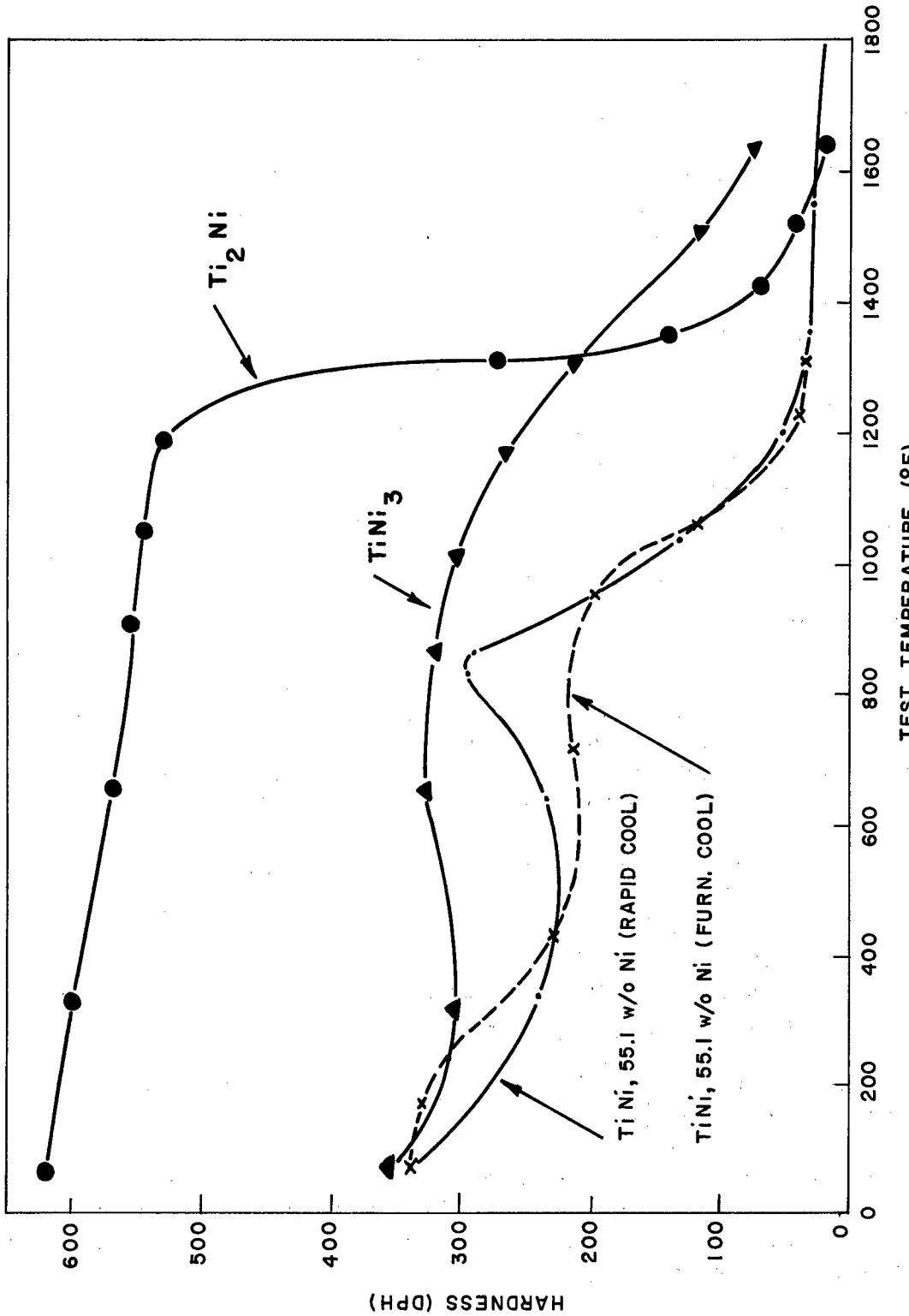

Fig. 16. Showing Hot Hardness Data on the Three Intermediate Phases of Nickel-Titanium.

REFERENCE RADIOGRAPHS OF THIN WALL STEEL CASTINGS FOR AEROSPACE APPLICATIONS

Steel castings are finding increased application in aerospace structural and propulsion components. However, before a full utilization of steel castings can be effected, the disparity in concepts of the foundry, the aerospace industries and the military as to what constitutes a sound casting must be reconciled. This will be accomplished by preparing comprehensive and realistic standards and specifications for the quality desired. A step in this direction has been taken through the preparation at the Naval Ordnance Laboratory of a set of thin wall steel casting reference radiographs to be used as a base for standards. The proposed document will illustrate the common steel casting discontinuities in several degrees of intensity. It will also contain illustrations of discrete and propagating discontinuities and a Glossary of Defects. Fig. 17 shows examples of discontinuities which will be illustrated. The illustrations will be designed for those castings 0.75 inch thick or less requiring high strength, good surface finish and close dimensional tolerances. Castings meeting these requirements are made by the shell mold, ceramicast, lost wax or frozen mercury process. They are frequently made from the following compositions: 4130, 300 and 400 series stainless and the super-alloys.*

The assistance of the aircraft industry was sought in determining necessary document contents and in supplying illustrative material, both castings and radiographs. When it was found that the supply of illustrative material obtainable from aircraft casting vendors lacked variety, resort to procurement of castings with specified defects was decided upon.

- - - - - - - - - - - -

* 4130 - A low alloy steel containing nominally 1.00% chromium and .25% molybdenum

300 Stainless - The series of stainless steels with chromium contents of from 16 to 20% and nickel from 7 to 10%. These steels are austenite and not capable of hardening by heat treatment.

400 Stainless - The series of stainless steels with chromium contents varying from 12 to 18%

Super-Alloys - A term applied to alloys with the highest available strength at elevated temperatures. They include alloys with high nickel, chromium and cobalt contents. Molybdenum, tungsten and columbium are other important alloying elements.

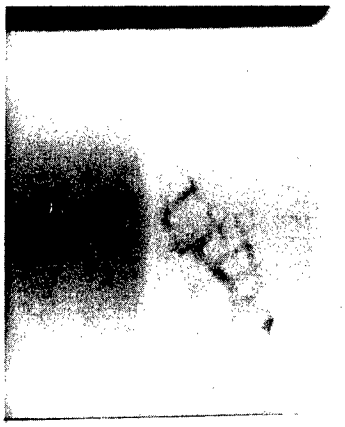

BRANCHING SHRINKAGE

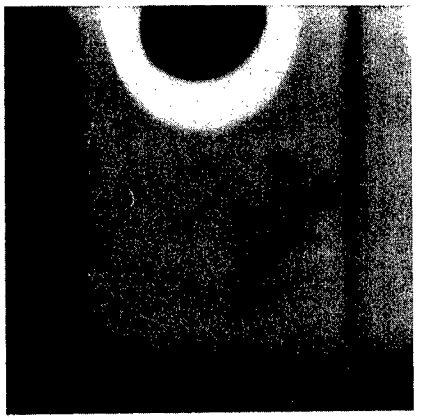

SPONGE SHRINKAGE

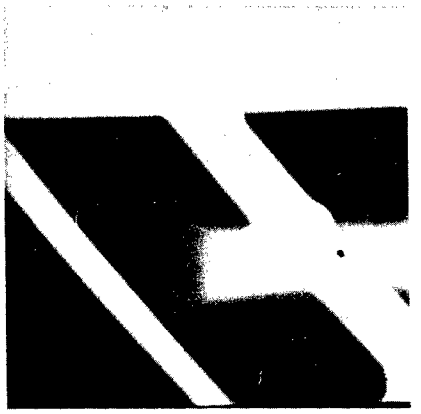

MOLD RIDGE

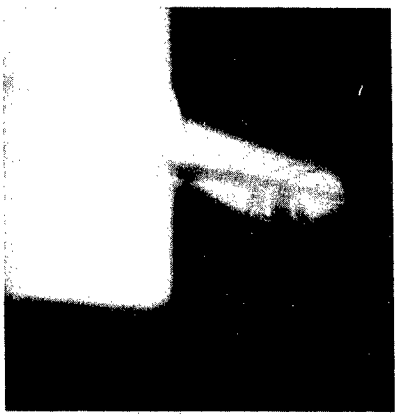

SHRINKAGE CAVITY

Fig. 17. Discontinuities in Steel Aircraft Castings.

Specifications for these castings were prepared and a contract was negotiated for their procurement. Liaison was established and technical assistance provided to guide the contractor in supplying suitable material for classification at NOL.

The cooperation of the American Society for Testing Materials (ASTM) was obtained for preparation of the proposed reference radiographs. To implement this participation, duties were assigned to an ASTM task group. These duties included review of illustrations prepared at NOL and assistance in compilation of the discontinuity nomenclature.

During 1960 approximately 70 percent of the document illustrations were provided. Table IV indicates the progress made in making the tentative graded defect selection. A rectangular chill technique and closely controlled pouring rates will be relied upon to fill the gaps in required branching shrinkage and shrinkage cavity illustration.

PROPERTIES OF WHISKERS

Whiskers are filamentary growths of materials with large length-to-diameter ratios. They are not something new, however, for they have been of scientific interest intermittently for the past 200 years. The most recent interest came in 1952, when Galt and Herring demonstrated that some whiskers had strengths (tensile and shear) approaching that calculated for perfect crystals. Since then whiskers of many organic and inorganic materials have been grown by various techniques. Their growth habits are of considerable interest and importance in the field of crystal growth. The mechanical properties of whiskers have received the most study, but some work has also been done on other physical properties such as electrical, magnetic, and surface properties.

Beryllium oxide whiskers and platelets were grown by heating beryllium metal in hydrogen at 1500°C for 16 hours. A new type of whisker called a "flagpole" whisker and consisting of a BeO whisker topped by a ball of beryllium metal, was found. A growth mechanism, in which the metal from the ball reacts with the oxygen in the atmosphere, forms the whisker, and pushes the ball away from the substrate, has been proposed. However, tentative studies by means of X-ray microradiography (Fig. 18) and by direct microscopic examination of the balls' interior have so far not substantiated the fact that those balls which are attached to whiskers are more porous than those which are not, as the growth mechanism suggests. X-ray diffraction and polarizing microscope studies gave the whisker axis as the crystallographic c-axis. Mechanical tests revealed that the whiskers could withstand strains in excess of 1%.

TABLE IV

GRADED DEFECT ILLUSTRATIONS AVAILABLE 31 DEC. 1960

Defect	Section Thickness	Tentative Grade *							
		1	2	3	4	5	6	7	8
Inclusions	.12			x	x	x	x	x	x
Less Dense	.37		x	x	x	x	x	x	x
	.75	x	x		x		x	x	x
Gas Holes	.12	x		x		x	x	x	x
	.37	x	x		x	x	x	x	x
	.75	x	x	x	x	x	x	x	x
Sponge Shrinkage	.12	x	x	x		x	x	x	x
	.37	x		x	x	x	x		x
	.75	x	x	x		x	x	x	x
Dendritic Shrinkage	.12	x	x	x	x	x	x	x	x
	.37	x	x	x				x	x
	.75	x	x	x	x	x			
Branching Shrinkage	.12						x		x
	.37								x
	.75	x	x	x			x	x	x
Shrinkage Cavity	.12	x	x			x	x		x
	.37	x	x		x	x	x	x	x
	.75	x				x			x

* Grade as given refers to the severity of the defect whose image appears in the radiographic illustration. The grades increase in severity from 1 to 8. The determination of a given grade and the number of grades has been arbitrary and based upon judgment.

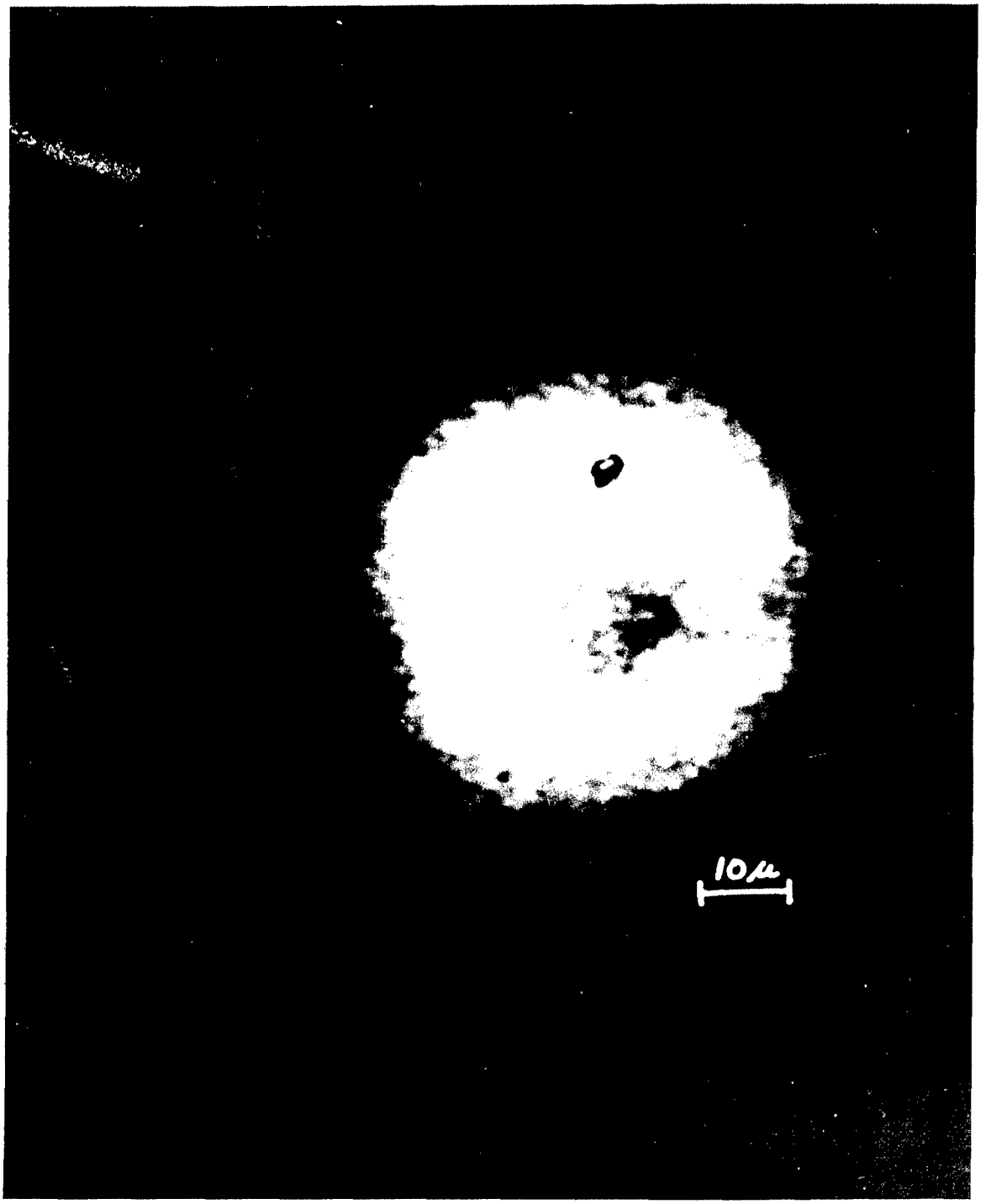

Fig. 18. Microradiographs of a ball from a flagpole whisker of BeO. Spot is a flow in the X-ray plate. Magnification: 1625 X.

"Flagpole" whiskers of aluminum oxide have also been grown using the same technique as that used for the beryllium oxide "flagpole" whiskers. But aluminum oxide whiskers were grown without balls which had preferential growth directions (Fig. 19). This was accomplished by growing the whiskers on oriented single crystal substrates.

X-RAY DIFFRACTION

X-ray diffraction in conjunction with polarized light optical observations, was used in the structural analysis of beryllium oxide (BeO) whiskers. These whiskers belong to the hexagonal crystal symmetry system. As is characteristic of many crystals, these specimens grew in several shapes. X-ray diffraction measurements indicated that most specimens grew with the c axis (0001) perpendicular to and the $(\bar{1}010)$ axis parallel to the whisker axis. However, a few whiskers had their c axis 60° from the whisker axis. In Fig. 20 is illustrated an example of a single whisker having both the c axis perpendicular to the whisker axis and suddenly changing to 60° toward the tip of the whisker. Platelets were also grown which were long in the same direction that the above whiskers were long, and the c-axis was found to be parallel to the width of the platelet.

ULTRASONIC STUDIES AT 1,000 Mc AND ABOVE

With the recent success in generating ultrasonic waves in the kilomegacycle region, a new field of ultrasonic investigation has been undertaken at this Laboratory. At present, using a frequency of 1,000 Mc, the resonance between phonons and spin waves, which occurs in magnetic materials when the energy and momentum of these waves become equal, is being studied. The interaction of the magnetization vector with the elastic strains (as observed in magnetostriction) is the cause of interesting non-reciprocal acoustic properties of the magnetic crystal. For example, when the elastic wave propagation vector and the magnetization lie along the same axis, circularly polarized shear waves of different senses have unequal velocities and attenuations. The effects of this coupling are most pronounced at frequencies and magnetic fields which correspond to this phonon-spin wave resonance.

To generate elastic waves at these frequencies, a thin quartz rod many wavelengths long was placed in such a manner that its tip protrudes into the high electric field portion of a re-entrant type cavity. Because of the ease at which the free end can move, an elastic wave is generated

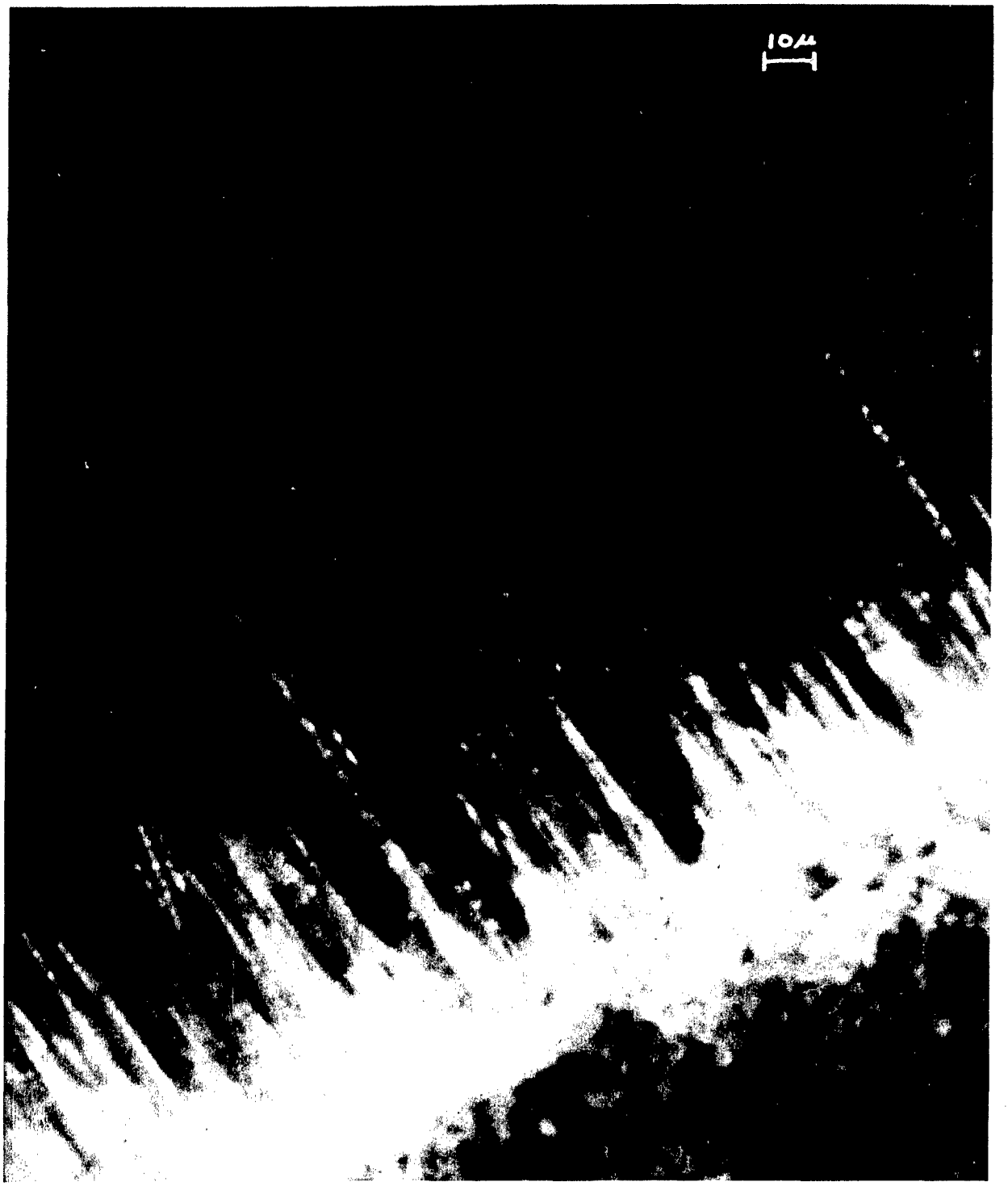

Fig. 19. Sapphire whiskers growing from an oriented sapphire single crystal disc. Magnification 955 X.

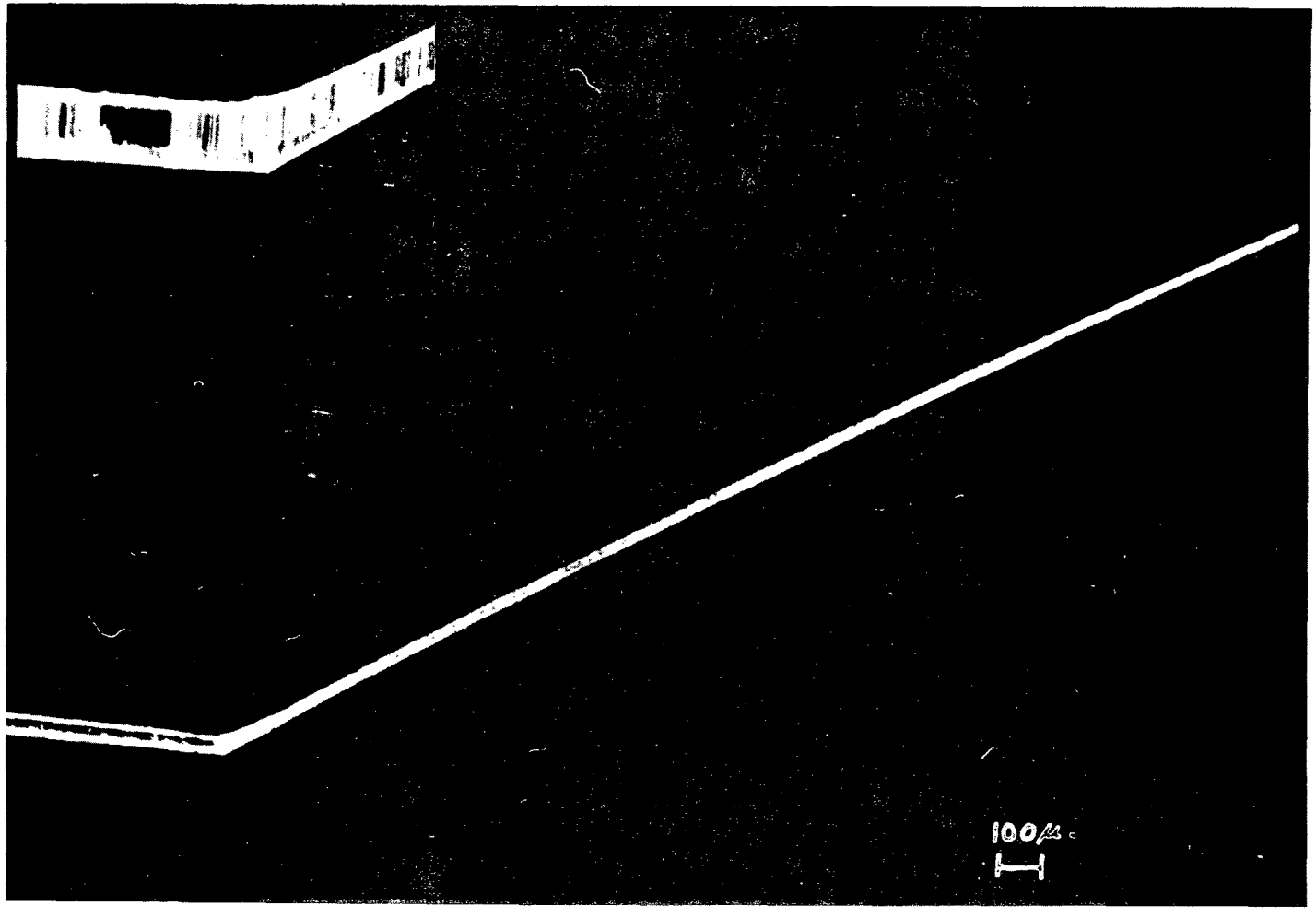

Fig. 20. This kinked whisker is an example of the c axis perpendicular to the whisker axis in the lower portion and the c axis suddenly changing to 60^{o} with the whisker axis toward the tip of the whisker. The magnified inset of the kinked portion shows the striations parallel to the c axis.

at the surface of the rod by means of the piezoelectric action of the quartz. A 1,000 Mc double re-entrant cavity, constructed as small as possible to allow it to be placed between the poles of a magnet, is shown in Fig. 21. Preliminary attenuation and velocity measurements made with this cavity in AC, BC, and X-cut quartz delay lines are in agreement with those made by other investigators. Attenuation in small or highly attenuating crystals is measured by cutting the crystal samples into small discs and sandwiching them between two similar quartz rods as shown in the figure. A thin film of indium metal on the flat surfaces of the sample and delay lines produces a thin but relatively strong bond when a slight pressure is applied to the sandwich for a short time. This bond is usable over the wide temperature range from room temperature to 4°K. After the technique of bonding crystalline quartz to the sample was understood, pulses of 1,000 Mc transverse elastic waves were transmitted through a BC-cut quartz-yttrium iron garnet-BC cut quartz sandwich at room temperature, 77°K and 4°K. The attenuation of this sample in these initial measurements did not appear to be a function of magnetic field strength or direction. In addition, apparatus to extend these measurements to 10 Kmc is being assembled.

LOW TEMPERATURE ULTRASONIC ATTENUATION IN FAST NEUTRON IRRADIATED FUSED SILICA

Low temperature ultrasonic attenuation measurements have been made in fused silica before and after heavy fast neutron irradiation. The purpose of this study was to obtain information about the mechanism responsible for the low temperature attenuation as related to the structure or defects of glass and the changes which occur as a result of the fast neutron bombardment. In addition, annealing studies were made on the irradiated sample in order to study the recovery of the irradiation-induced attenuation change as a function of temperature.

A broad attenuation curve (as illustrated in Fig. 22), attributed to a structural relaxation with a distribution of activation energies, occurs at low temperatures. The shape of the loss curve is dependent upon the distribution of activation energies while the amplitude is proportional to the number of structural units which contribute to the relaxation process. A heavy fast neutron irradiation produced no change in the shape of the curve while the amplitude decreased considerably. A damaging mechanism which either inactivates or does not noticeably affect the contributing units is indicated. In addition to point defects produced by displacement collisions, thermal spikes with temperatures above the softening point of fused silica, lasting on the order of 10^{-12} seconds

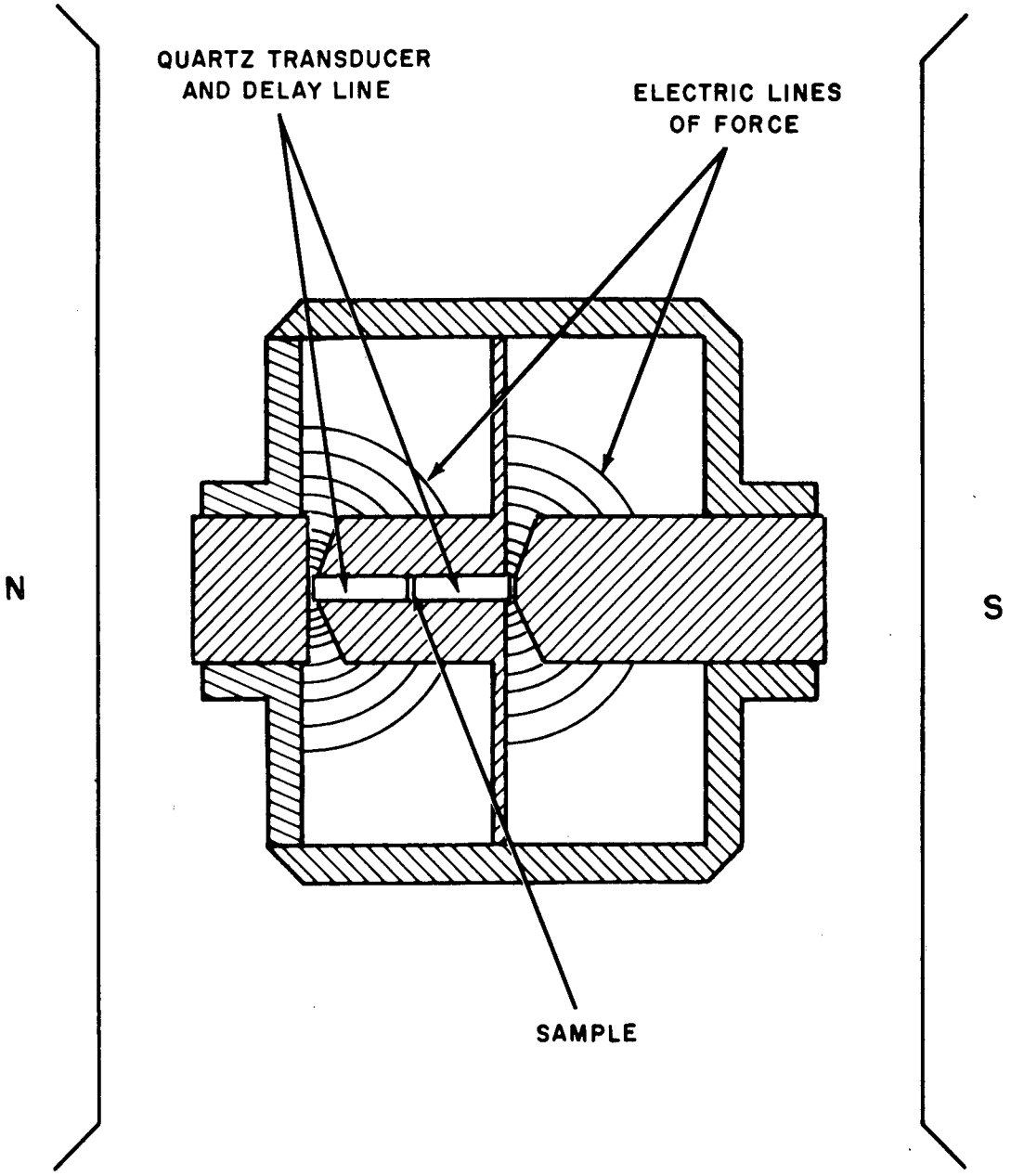

Fig. 21. Cavity for generation and detection of 1,000 Mc elastic waves

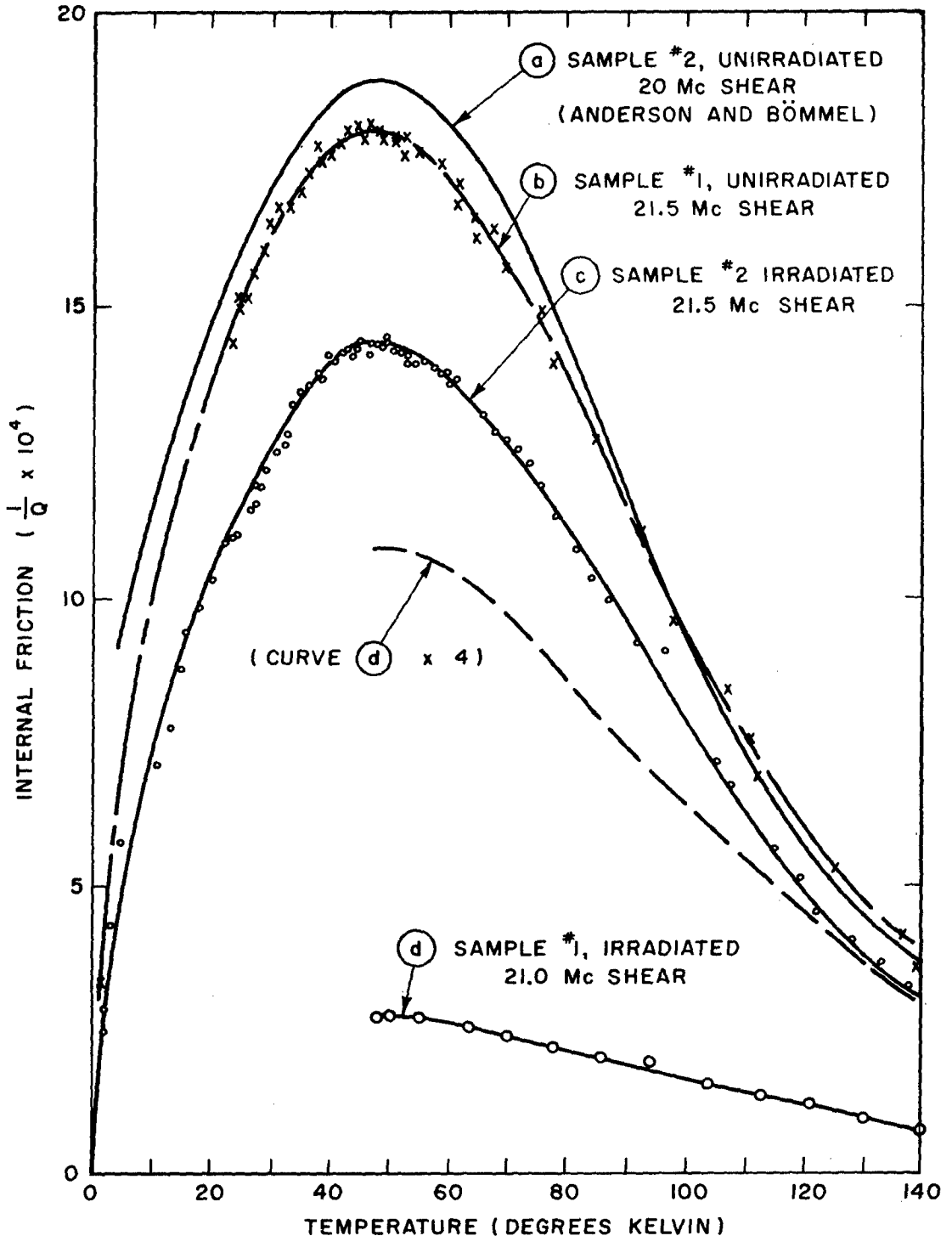

Fig. 22. Comparison of internal friction in two samples of fused silica before and after heavy fast neutron irradiation (>5 x 10^{19} neutrons/cm^2) using shear waves.

and having radii of the order of 10 Angstroms, are a possible cause of the irradiation-induced damage. A relaxation loss mechanism associated with a non-impurity defect appears to be consistent with the results of this study.

EFFECT OF IMPURITIES ON TRANSFER OF VIBRATIONAL ENERGY IN LIQUIDS

The cause of an ultrasonic loss in non-associated liquids has been shown to be due to a thermal relaxation effect. In liquid carbon disulfide this involves a transfer of energy between the vibrational and translational degrees of freedom. In accounting for the temperature and pressure dependence of the vibrational relaxation time of liquid carbon disulfide, it appeared that only binary collisions were important. A complete study of the problem of collisions between like molecules was made by examining the relaxation time of carbon dioxide from the gas to the liquid state. The conclusion was that binary collisions were responsible for the transfer of energy in the gas and liquid, and that there was very little difference in the vibrational relaxation mechanism in the two states. The next step in this study was to compare further the mechanism of vibrational energy transfer by investigating the effect of impurities, that is, the effect of collisions between unlike molecules on the vibrational relaxation time in liquid carbon disulfide.

Ultrasonic attenuation measurements were made in liquid carbon disulfide at a temperature of 25°C. From this measurement the relaxation frequency and relaxation time of the liquid were calculated. Further measurements were made when methyl, propyl, and butyl alcohol were added in concentrations up to .06 mole per cent. In each case the relaxation frequency was increased linearly with the amount of impurity added, (see Fig. 23). The relaxation frequency of the pure carbon disulfide was 78.0 Mc. The shifts in relaxation frequency of liquid carbon disulfide at 25°C caused by the impurities added are:

Methyl Alcohol	107 Mc/mole per cent
Propyl Alcohol	255 Mc/mole per cent
Butyl Alcohol	318 Mc/mole per cent

The effective collision efficiency, (f_{AB}/f_{AA}),--the shift in relaxation frequency of the mixture for a known concentration, divided by the relaxation frequency of the pure substance -- for the liquid was compared to the collision efficiency for gaseous carbon disulfide containing the same impurities. The results showed that $(f_{AB}/f_{AA})_{liq} = (f_{AB}/f_{AA})_{gas}$ within experimental error.

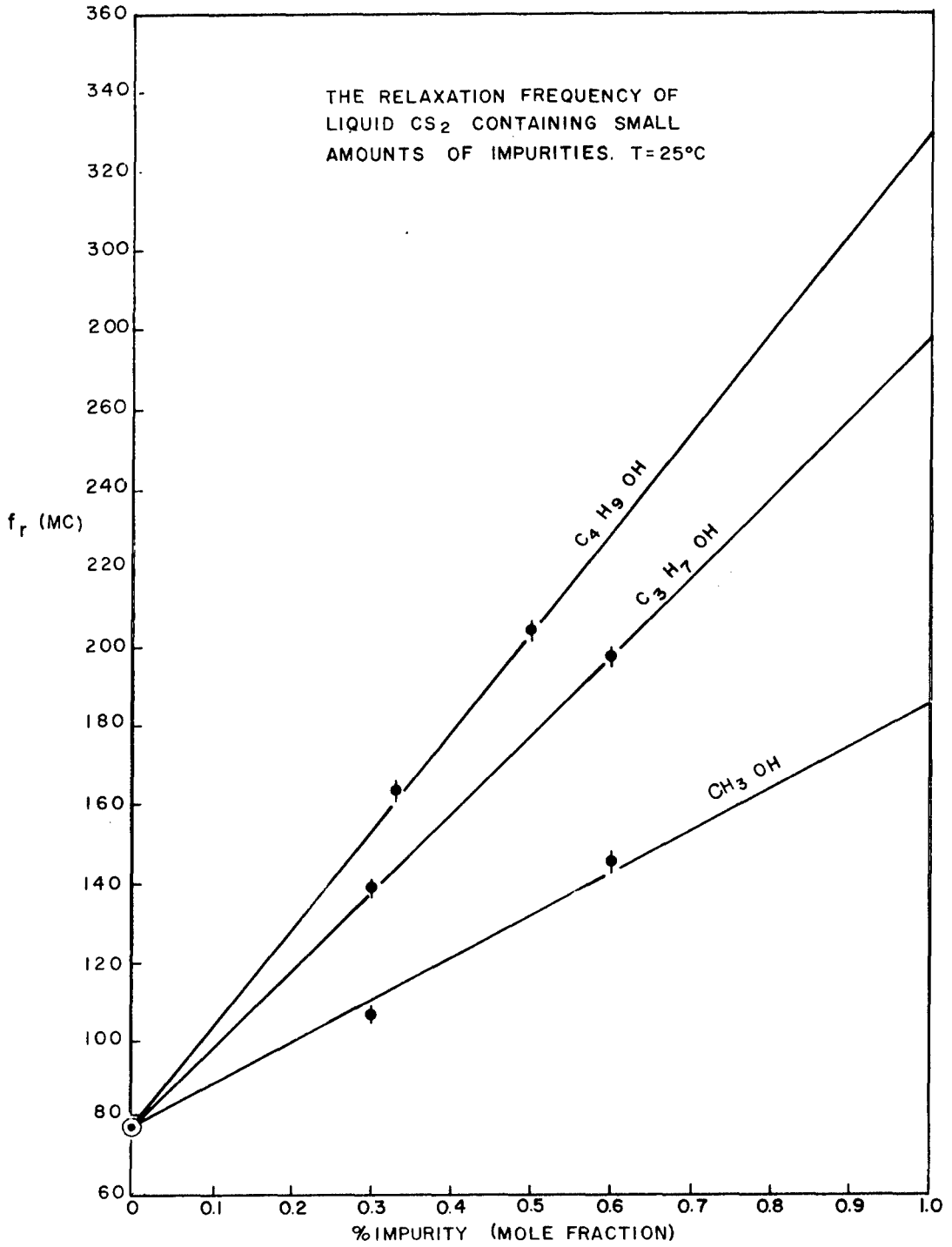

Fig. 23. Relaxation frequency of liquid CS_2 containing small amounts of impurities of methyl, propyl and butyl alcohol. T = 25°C.

This experiment shows that the unlike collision process in the liquid state has the same mechanism as the unlike collision process in the gas state.

REPORTS AND PUBLICATIONS

Naval Ordnance Laboratory Reports

Adams, C. Q. - "New Flux-Gate Magnetometers for Use With Single-Strip Permeameters", NavOrd Report 6835, 21 March 1960

Allgaier, R. S. - "The 1960 International Conference on Semiconductor Physics at Prague: The Lead Salt Semiconductors PbS, PbSe, and PbTe, and Other Selenides and Tellurides," NavWeps Report 7332, 18 October 1960

_____, (See Stern, F.)

Alperin, Harvey A. - "A Neutron Diffraction Study of Nickel Oxide," NavOrd Report 6907, 14 June 1960

Dixon, J. R. - (See Stern, F.)

Enright, D.P. - "Properties of Magnesium-Doped Indium Arsenide," NavOrd Report 6814, 1 Feb 1960

Feinberg, I.J., Criscuolo, E. L., and Youshaw, R.A., - "Reference Radiographs for Steel Aircraft Castings - Progress in Preparation, July 1958 - December 1959" NavOrd Report 6811, 18 Feb 1960

Greene, R. F. - "Theory of Surface Thermoelectricity," NavOrd Report 6924, July 1960

Haben, J. - "Evaluation of Supermendur Cut Cores for an Electromagnetic Transducer," NavWeps Report 7337, 4 November 1960

Helms, H.H. - "Adaptability of Iron-Silicon Magnetic Alloys for Special Environments," NavWeps Report 7331, 26 October 1960

Norr, M. K. - "A Kinetic Study of the Lead-Thioureau Reaction. II," NavWeps Report 7340, 17 October 1960

Stern, F., Allgaier, R. S., Dixon, J. R., Zemel, J.N., - "Report of Travel to the 1960 International Conference on Semiconductor Physics," NavWeps Report 7321, 30 September 1960

Thomas, Ethel G. - "IBM Fortran Program for Evaluating Semiconductor Surface Transport Integrals," NavOrd Report 6754, December 1960

Zemel, J.N. (See Stern, F.)

Papers and Abstracts Published

Adams, C. Q. - "A Simple Field Detector for a D-C Permeameter," Rev. Sci. Instr. 31, 1119 (1960)

Allgaier, R.S. - "Weak-Field Magnetoresistance in p-Type Lead Telluride at Room Temperature and 77°K," Phys. Rev. 119, 554-561 (1960)

_____, Burke, J.R. - "Magnetic Field Dependence of the Hall Coefficient in p-Type PbTe," Bull. Am. Phys. Soc. 5, 152 (1960)

_____, "Magnetoresistance and the Band Structure of PbS, PbSe and PbTe," Bull. Am. Phys. Soc. 5, 289 (1960)

_____, (See Brebrick, R. F.)

Alperin, H.A. - "Neutron Diffraction Investigation of the Magnetic Structure of Nickel Oxide," J. Appl. Phys. 31, 354S (1960)

_____, and S. J. Pickart - "Evidence for Tetrahedral Site Ordering in $Mn_{0.6}Fe_{2.4}O_4$," Bull. Am. Phys. Soc. 5, 458 (1960)

_____, (See Pickart, S.J.)

Brebrick, R. F. - "Composition Stability Limits of Binary Semiconductor Compounds," Bull. Am. Phys. Soc. 5, 263 (1960)

_____, Allgaier, R.S. - "Composition Limits of Stability of PbTe," J. of Chem. Phys., 32, 1826-1831 (1960)

Burke, J. R. - (See Allgaier, R.S.)

Callen, E. R. - "Anisotropic Magnetization," J. Appl. Phys. 31, 149S (1960)

_____, "Ordering Effects in Iron-Rich Manganese Ferrite," Bull. Am. Phys. Soc. 5, 458 (1960)

_____, and H. B. Callen - "Anisotropic Magnetization," J. Phys. Chem. Solids, 16, 310 (1960)

Dayhoff, E. S. - "Theory of Diffraction in Microwave Interferometry," Nat'l Bureau of Standards Journ. of Research 64B, 1 (1960; also NBS Report 6068 (D.M. Kerns and E. S. Dayhoff)

Edwards, P.L. - "Rolling O-Ring Seal," Rev. Sci. Instr. 31, 1356 (1960)

_____, and R. J. Happel, Jr. - "Beryllium Oxide 'Flagpole' Whiskers," Bull. Am. Phys. Soc. 5, 49 (1960)

Gordon, D. I. - "Magnetic Cores and Permanent Magnets in Hyper-Environments," Proceedings of Institute of Environmental Sciences National Meeting, April 1960, Los Angeles (Inst. Environmental Sciences, Mt. Prospect, Ill.) pp 205-228

_____, and Sery, R.S. - "Nuclear Irradiation Effects on Ferromagnetic Core Materials," Solid State Physics in Electronics and Telecommunications - Proceedings of an International Conference Held in Brussels, June 2-7, 1958, edited by M. Désirant and J. L. Michiels (Academic Press, London, 1960, Vol. 4, pp 824-858

Greene, R. F. - "Surface Transport Theory," J. Phys. Chem. Solids, 14, 291 (1960)

_____, Frankl, D. R., and Zemel, J.N. - "Surface Transport in Semiconductors," Phys. Rev. 118, 967-975 (1960)

Happel, R. J., Jr. - (See Edwards, P.L.)

Houston, B.B. and Norr, M.K. - "Dislocation Etch Pits on p-Type Lead Telluride," J. Appl. Phys. 31, 615-616 (1960)

_____, "Growth of Lead Telluride Crystals by the Czochralski Method," Bull. Am. Phys. Soc., 5, 166 (1960)

Litovitz, T. A. (See Madigosky, W.M.)

_____, (See Slie, W.M.)

Lundsten, R. H. (See Pasnak, M.)

Madigosky, W.M., and T. A. Litovitz - "Mean Free Path and Ultrasonic Vibrational Relaxation in Liquids and Dense Gases," J. Acoust. Soc. Am. 32, 928 (1960)

McGuire, T. R. - "Magnetic Susceptibility of a Chromium Single Crystal," Bull. Am. Phys. Soc. 5, 456 (1960)

_____, and R. R. Heikes - "Magnetic Properties of the $Li_xMn_{1-x}Se$ System," J. Appl. Phys. 31, 276S (1960)

_____, and S. W. Greenwald - "Substitution of Chromium in Ferrites," Solid State Physics in Electronics and Telecommunications (Academic Press, 1960)

Norr, M. K. (See Houston, B.B.)

Pasnak, M. and Lundsten, R.H. - "Effects of Ultra-High Temperature on Magnetic Properties of Core Materials," Communication and Electronics No. 46, 1033 (1960)

_____, and Lundsten, R. H. - "The Ferrotracer for Dynamic B-H Loops," Elec. Mfg. 66 (No. 3), 174 (Sept. 1960)

Pickart, S. J. - "Magnetic Structure of $MnCO_3$," Bull. Am. Phys. Soc. 5, 59 (1960

_____, "Antiferromagnetic Ordering in $FeCo_3$," Bull. Am. Phys. Soc. 5, 357 (1960)

_____, and R. Nathans - "Magnetic-Form Factor of Fe_3Al," J. Appl. Phys. 31, 372S (1960)

_____, "Study of Rhombohedral V_2O_3 by Neutron Diffraction, "J. Chem. Phys. 32, 308 (1960) (A. Paoletti and S. J. Pickart)

_____, "Neutron-Diffraction Study of Ti_2O_3," J. Phys. Chem. Solids 13, 167 (1960) (G. Shirane, S. J. Pickart and R. Newnham)

_____, "3d Electron Distributions in Fe_3O_4 from Polarized Neutron Measurements," Bull. Am. Phys. Soc. 5, 455 (1960) (R. Nathans, S. J. Pickart and H. A. Alperin)

_____, (See Alperin, H.A.)

Scanlon, W.W. - "Semiconductor Research in the Navy," Journal of Metals, Aug. 1960

_____,"Stoichiometry in Compound Semiconductors," Metallurgical Society Conference, Vol. 5, Properties of Elemental and Compound Semiconductors, p 185 (1960) Edited by Harry C. Gatos

_____, "Stoichiometry in Semiconductors," Symposium on Solid State and Plasma Physics, 3-4 Nov. 1959, the Johns Hopkins Univ., Radiation Laboratory, Baltimore, Md., Technical Report No. AF-73 (Jan. 1960)

Sery, R. S. (See Gordon, D. I.)

Slie, W. M., and Litovitz, T. A. - "Effects of Alcohol on the Vibrational Relaxation in Liquid CS_2," J. Acoust. Soc. Am. 32, 1510 (1960)

Stern, F. - "Atomic Scattering Factor in Iron," Bull. Am. Phys. Soc., 5, 169 (1960)

_____, "3d Form Factor in Metallic Iron," Bull. Am. Phys. Soc. 5,456 (1960)

Strakna, R. E. - "Ultrasonic Attenuation in Fast Neutron Irradiated Fused Silica at Low Temperatures," Bull. Am. Phys. Soc. 5, 26 (1960)

Varela, J. O. (See Zemel, J. N.)

Wangsness, R. K. - "Ferrimagnetic Resonance in Three-Sublattice Systems," Phys. Rev. 119, 1496 (1960)

Zemel, J. N., Editor - Proceedings of Second Conference on Semiconductor Surfaces, Pergamon Press, (1960)

_____, Zemel, J. N. (See Greene, R. F.)

_____, Varela, J. O., "Surface Properties of PbS Photoconductors," J. Phys. Chem. Solids, 14 p. 142 (1960)

PAPERS PRESENTED AT MEETINGS OUTSIDE THE LABORATORY

In the United States

Alperin, H. A. - "Application of Neutron Diffraction to the Study of Antiferromagnetism," University of Connecticut Physics Colloquium, 1 April 1960

_____, and S. J. Pickart - "Evidence for Tetrahedral Site Ordering in $Mn_{0.6}Fe_{2.4}O_4$," Conference on Neutron Diffraction in Relation to Magnetism and Chemical Bonding, Gatlinburg, Tennessee, 20-22 Apr 1960

_____, "Electron Spin Configuration in NiO" and "Long Range Ordering in Ferrites," Meeting of the Office of the Director of Defense Research and Engineering, Advisory Group on Electronic Parts, Brookhaven National Laboratory, 8-9 September 1960

_____, (See Pickart, S.J.)

Allgaier, R. S., Burke, J. R., "Magnetic Field Dependence of the Hall Coefficient in p-Type PbTe," American Physical Society Meeting, Detroit, Michigan, 21-24 March 1960

_____, "Magnetoresistance and the Band Structure of PbS, PbSe and PbTe," American Physical Society Meeting, Washington, D. C., 25-28 April 1960 (Invited paper)

Brebrick, R.F. - "Composition Stability Limits of Binary Semiconductor-Compounds," American Physical Society Meeting, Washington, D. C., 25-28 April 1960; Semiconductor Research Group, IBM Lab., Poughkeepsie, N.Y., 16 May 1960; Gordon Research Conference on the Chemistry and Metallurgy of Point Defects, Meriden, N.H., 25-29 July 1960; and Lincoln Labs., M.I.T., Lexington, Mass., 4 October 1960

_____, "Chemistry of Semiconductors," Lectures at Georgetown University Graduate Summer School of Physical Chemistry, Washington, D. C., 11-13 July 1960

Burke, J. R., (See Allgaier, R.S.)

Callen, E. R. - "Anisotropic Magnetization," Naval Research Laboratory Physics Department Seminar, 18 Jan. 1960

_____, "Magnetism," Johns Hopkins University Chemistry Department Colloquium, 9 March 1960

_____, "Temperature Dependent Hamiltonians in Ferromagnetism," National Bureau of Standards Statistical Mechanics Seminar, 30 March 1960

_____, "Ordering Effects in Iron-Rich Manganese Ferrite," Conference on Neutron Diffraction in Relation to Magnetism and Chemical Bonding, Gatlinburg, Tennessee, 20-22 April 1960

_____, "Anisotropic Curie Temperature," Sixth Annual Conference on Magnetism and Magnetic Materials, New York, 14-17 Nov. 1960

Dixon, J. R. - "Solids in Action - Using Their Electrical, Optical and Thermal Properties," Commerce Auditorium, Washington, D.C., (part of a lecture series "Materials Development in the Space and Atomic Age," sponsored by the National Bureau of Standards and five technical societies for high school groups)

_____, "Solid State Physics Research," Research Club of Woodrow Wilson High School, 25 Feb. 1960

Edwards, P. L., and R. J. Happel, Jr. - "Beryllium Oxide 'Flagpole' Whiskers," American Physical Society Meeting, New York, 27-30 Jan. 1960

Gordon, D. I. - "Magnetic Cores and Permanent Magnets in Hyper-Environments," Institute of Environmental Sciences National Meeting, Los Angeles, Calif., 6-8 April 1960

Greene, R. F. - "Electrical Transport and Semiconductor Surfaces," Univ. of Utah, Salt Lake City, 14 October 1960

Happel, R. J. Jr. - (See Edwards, P.L.)

Houston, B.B. - "Growth of Lead Telluride Crystals by the Czochralski Method," American Physical Society Meeting, Detroit, Michigan, 21-24 March 1960

Litovitz, T. A. - (See Madigosky, W.M.)

_____, (See Slie, W.M.)

Madigosky, W.M. and T. A. Litovitz - "Mean Free Path and Ultrasonic Vibrational Relaxation in Liquids and Dense Gases," 59th Meeting of the Acoustical Society of America, Providence, R. I., 9-11 June 1960

Maxwell, L. R. - "Magnetic Atoms Amongst Others," Retiring Presidential Address. Philosophical Society of Washington.

McGuire, T. R. - "Magnetic Susceptibility of a Chromium Single Crystal," Conference on Neutron Diffraction in Relation to Magnetism and Chemical Bonding, Gatlinburg, Tennessee, 20-22 April 1960

Pickart, S. J. - "Magnetic Structure of $MnCO_3$," American Physical Society Meeting, New York, 27-30 January 1960

_____, 3d Electron Distributions in Fe_3O_4 from Polarized Neutron Measurements," Conference on Neutron Diffraction in Relation to Magnetism and Chemical Bonding, Gatlinburg, Tennessee, 20-22 April 1960 (R. Nathans, S. J. Pickart and H. A. Alperin)

_____, "Antiferromagnetic Ordering in $FeCO_3$," American Physical Society Meeting, Montreal, Canada, 15-17 June 1960

_____, "Magnetic Structure Transitions in $Li_xMn_{1-x}Se$ Involving Double Exchange," "Magnetic Structure of Antiferromagnetic $MnTiO_3$, $NiTiO_3$, $FeTiO_3$ and Solid Solutions of $FeTiO_3$ and α-Fe_2O_3," and "Magnetic Structure of Chromium Substituted Spinels," Meeting of the Office of the Director of Defense Research and Engineering, Advisory Group on Electronic Parts, Brookhaven National Laboratory, 8-9 September 1960

Scanlon, W. W. - "Semiconductor Research at the Naval Ordnance Laboratory," Naval Research Laboratory, 18 Feb. 1960

_____, "Large Atomic Number Semiconductors," Nuclear Detection Conference, Ashville, North Carolina, 29 Sept 1960

_____, "Research on Photoconductivity," Navy Industrial Clinic, Univ. of Minnesota, Minneapolis, Minn., 19 Oct. 1960

_____, "Thermoelectricity," National Academy of Sciences, National Research Council, Washington, D. C., Jan. 1960

Slie, W. M., and T. A. Litovitz - "Effects of Alcohol on the Vibrational Relaxation in Liquid CS_2," 60th Meeting of the Acoustical Society of America, San Francisco, Calif., 20-22 Oct. 1960

Stern, F. - "Atomic Scattering Factor in Iron," American Physical Society Meeting, Detroit, Michigan, 21-24 March 1960

_____, "3d Form Factor in Metallic Iron," Conference on Neutron Diffraction in Relation to Magnetism and Chemical Bonding, Gatlinburg, Tenn., 20-22 April 1960

_____, "Calculation of Optical Absorption in Intermetallic Semiconductors," Solid State Seminar, Naval Research Lab., Washington, D.C., 14 Nov. 1960

_____, "The Electronic Energy Band Structor of Iron," Metallurgy Div., National Bureau of Standards, Washington, D. C., 14 Dec. 1960

Strakna, R. E. - "Ultrasonic Attenuation in Fast Neutron Irradiated Fused Silica at Low Temperature," American Physical Society Meeting, New York, 27-30 Jan. 1960; also, University of Connecticut Physics Department Seminar, 11 March 1960

In Foreign Countries

Allgaier, R. S. - "Galvanomagnetic Effects and Band Structure in PbS, PbSe, and PbTe," International Conference on Semiconductor Physics, Prague, Czechoslovakia, 29 Aug - 2 Sept. 1960; Seminar of Division of Pure Physics, National Research Council, Ottawa, Canada, 30 May 1960

Dixon, J. R. - "Optical Absorption Mechanisms in Indium Arsenide," International Conference on Semiconductor Physics, Prague, Czechoslovakia, 29 Aug - 2 Sept 1960

Greene, R. F. (See Zemel, J.N.)

Stern, F. - "Calculation of Optical Absorption in III-V Semiconductors," International Conference on Semiconductor Physics, Prague, Czechoslovakia, 29 Aug. - 2 Sept. 1960

Zemel, J. N. and Greene, R. F. - "Semiconductor Surface Transport," International Conference on Semiconductor Physics, Prague, Czechoslovakia, 29 Aug.-2 Sept. 1960

DISTRIBUTION

	COPIES
Chief, Bureau of Naval Weapons Navy Department, Washington 25, D. C. Attn: Technical Library (DLI-31)	2
R-12 (Dr. E. S. Lamar)	1
RM-13	1
RM-11 (S. J. Raff)	1
RRMA	1
RMWC-51 (M. Goldberg)	1
RRRE-2 (J. F. Dibrell)	1
RRRE-3 (M. J. West)	1
RU	
Chief, Bureau of Ships Navy Department, Washington 25, D. C. Attn: C. H. Hunt (Code 687C)	1
J. M. Kerr (Code 691B)	1
C. S. Woodside (Code 687C)	1
A. H. Young, Semiconductor Unit (Code 691A2)	1
Office of Naval Research Navy Department, Washington 25, D. C. Attn: Material Sciences Division (Code 419)	1
Commanding Officer Office of Naval Research Branch Office 495 Summer Street Boston 10, Massachusetts Attn: T. B. Dowd	1
Commanding Officer Office of Naval Research Branch Office 86 E. Randolph Street Chicago 1, Illinois Attn: Lloyd A. White	1
Commanding Officer Office of Naval Research, Pasadena Branch 1030 East Green Street Pasadena 1, California Attn: Technical Library	1

Director, U. S. Naval Research Laboratory
Washington 25, D.C.
Attn: Library (Code 2027 — 1
Code 7350 — 1
Code 6450 — 1
Code 6470 (R. Wallis) — 1

Commander, U. S. Naval Ordnance Test Station
China Lake, California
Attn: Technical Library — 1

Commanding Officer, U. S. Naval Ordnance Laboratory
Corona, California
Attn: Library — 1
R. F. Potter — 1

Commanding Officer and Director
U. S. Navy Electronics Laboratory
San Diego 52, California
Attn: Library — 1

Office of Director of Defense Research and Engineering
Washington 25, D. C.
Attn: Materials Division — 1

Directorate of Solid State Sciences
Air Force Office of Scientific Research
Washington 25, D.C. — 1

Headquarters, U. S. Air Force
Washington 25, D. C.
Attn: AFDRD-RD — 1

Hq. Detachment 2, Air Force Research Division (ARDC)
U. S. Air Force, Laurence G. Hanscom Field
Bedford, Massachusetts
Attn: CRRPL-3 — 1

Commanding General, Frankford Arsenal
Philadelphia 37, Pennsylvania
Attn: Library, Reports Section, #0270 — 1

Office of the Chief Signal Officer
Research and Development Division, Washington 25, D. C.
Attn: Signal Research Office — 1

Commanding Officer, Diamond Ordnance Fuze Laboratories
Washington 25, D.C.
Attn: Technical Reference Br. (ORDTL 012) 1

National Aeronautics and Space Administration
1520 H Street, N.W.
Washington 25, D. C.
Attn: Library/BIL 7

National Aeronautics and Space Administration
Lewis Research Center
21000 Brookpark Road
Cleveland 35, Ohio
Attn: Library 1

Director, National Security Agency
Fort George G. Meade, Maryland
Attn: Capt. A. M. Cole (REMP-2) 1
Miss Savakinas (CREF-332) Rm. 2C087 1

National Bureau of Standards
Washington 25, D. C.
Attn: Library 1
H. P. Frederikse 1

ASTIA (TIPCR)
Arlington Hall Station
Arlington 12, Virginia 10

Argonne National Laboratory
9700 South Cass Avenue
Argonne, Illinois
Attn: Hoylande D. Young 1

Armour Research Foundation
Chicago 16, Illinois
Attn: James J. Brophy (Asst. Mgr., Physics Research) 1

Brookhaven National Laboratory
Upton, Long Island, New York
Attn: Research Library 1
S. J. Pickart, Physics Dept. 1
H. A. Alperin, Physics Dept. 1

University of Arizona
Department of Physics
Tucson, Arizona
Attn: Roald K. Wangsness 1

Department of Physics
Carnegie Institute of Technology
Pittsburgh 13, Pennsylvania
Attn: Library 1

Documents Department
General Library
University of California
Berkeley 4, California 1

University of California
La Jolla, San Diego, California
Attn: W. Kohn, Department of Physics 1

Cornell University
Ithaca, New York
Attn: L. G. Parratt, Chairman, Dept. of Physics 1

George Washington University
Washington, D. C.
Attn: T. P. Perros, Chemistry Department 1

Gordon McKay Library, Harvard University
Division of Engineering and Applied Physics
Pierce Hall, Oxford Street
Cambridge 38, Massachusetts
Attn: Technical Reports Collection 1

Documents Division - ML
University of Illinois Library
Urbana, Illinois 1

University of Illinois
Urbana, Illinois
Attn: R. J. Maurer, Dept. of Physics 1

Applied Physics Laboratory, Johns Hopkins University
8621 Georgia Avenue
Silver Spring, Maryland
Attn: G. L. Seielstad, Supervisor, Tech. Repts. Grp. 1
C. K. Jen 1

Radiation Laboratory, Johns Hopkins University
1315 St. Paul Street
Baltimore, Maryland 1

University of Maryland
Department of Physics
College Park, Maryland
Attn: Richard Ferrell 1

Lincoln Laboratory
Massachusetts Institute of Technology
Box 73, Lexington 73, Massachusetts
Attn: Library, A-229 1
B. Lax 1

Massachusetts Institute of Technology
Cambridge 39, Massachusetts
Attn: Wayne B. Nottingham, Rm. 6-205 1
Laboratory for Insulation Research, Rm. 4-244 1
Research Laboratory of Electronics, Rm. 26-327 1

University of Rochester
Rochester 20, New York
Attn: D. L. Dexter, Institute of Optics 1

Texas Christian University
Physics Department
Fort Worth, Texas
Attn: Prof. P. L. Edwards 1

American Optical Company, J. W. Fecker Division
6592 Hamilton Avenue
Pittsburgh 6, Pennsylvania
Attn: W. Lewis Hyde 1

American Optical Company, Research Center
Southbridge, Massachusetts
Attn: Library 1

Avco Manufacturing Corporation Research Laboratories
2385 Revere Beach Parkway
Everett 49, Massachusetts 1

Baird-Atomic, Inc.
33 University Road
Cambridge 38, Massachusetts
Attn: Library 1

Battelle Memorial Institute
Columbus 1, Ohio
Attn: A. C. Beer, Solid State Physics 1

Bausch & Lomb Optical Co.
635 St. Paul Street
Rochester, New York
Attn: Dr. Foster 1

Bell Telephone Laboratories
Murray Hill, New Jersey
Attn: J. A. Morton 1

Bendix Aviation Corp.
Systems Division
Ann Arbor, Michigan
Attn: Lloyd G. Mundie 1

Clevite Research Center
540 East 105th Street
Cleveland 8, Ohio
Attn: Hans Jaffe, Electronic Research Division 1

E. I. duPont de Nemours & Co.
Photo Products Department
Parlin, New Jersey
Attn: Library 1

Eastman Kodak Company
App. and Optical Division
400 Plymouth Ave. N.
Rochester 4, New York
Attn: E. D. McAlister 1

Eastman Kodak Company
Navy Ordnance Division
50 West Main Street
Rochester 14, New York
Attn: G. J. Koch 1

Minnesota Mining and Manufacturing Company
2031 Hudson Road
St. Paul 6, Minnesota
Attn: Library 1
F. A. Hamm 1

Pacific Semiconductors, Inc.
10451 West Jefferson Blvd.
Culver City, California
Attn: H. Q. North 1

Parma Research Laboratory
Union Carbide Corporation
P. O. Box 6116
Cleveland 1, Ohio
Attn: R. G. Breckenridge 1
Library 1

Patterson, Moos
Division of Universal Winding Co., Inc.
90-29 Van Wyck Expressway
Jamaica 18, New York
Attn: Library 1
H. C. Lieb 1

Philco Corporation
Tioga and C Streets
Philadelphia 34, Pennsylvania
Attn: Research Library 1

Philips Laboratories
Irvington-on-Hudson, New York
Attn: Library 1
E. S. Rittner 1

Polaroid Corporation
730 Main Street
Cambridge 39, Massachusetts
Attn: R. Clark Jones 1

Radio Corporation of America Laboratories
Princeton, New Jersey
Attn: Library 1
S. Larach 1

Thomas A. Edison Research Laboratory	1
East Orange, New Jersey	
Attn: Research Library	1
D. H.Howling	1
General Ceramics Corporation	
Keasbey, New Jersey	
Attn: E. J. Hurst	1
General Electric Research Laboratory	
Schenectady, New York	
Attn: L. Apker	1
John R. Eshbach	1
E. M. Pell	1
R. W. Schmitt	1
General Motors Technical Center	
Physics Department, Research Laboratories	
12 Mile and Mount Roads	
Warren, Michigan	
Attn: Carl E. Bleil	1
Robert Herman	1
General Telephone and Electronics Laboratories, Inc.	
Bayside 60, New York	
Attn: P. H. Keck	1
H. F. Mayburg	1
Library	1
International Business Machines Corporation	
Research Center	
Yorktown, New York	
Attn: J. Samuel Smart	1
L. P. Hunter	1
J. F. Woods	1
ITT Laboratories	
3702 E. Pontiac Street	
Fort Wayne, Indiana	
Attn: Donald K. Coles	1
P. R. Mallory & Co., Inc.	
3029 E. Washington Street	
Indianapolis 6, Indiana	
Attn: Margaret Holtman, Librarian	1

Raytheon Manufacturing Company
1st Avenue
Needham, Massachusetts
Attn: R. J. Carney 1

Raytheon Manufacturing Company
150 California Street
Newton, Massachusetts
Attn: Library 1

Santa Barbara Research Center
Goleta, California
Attn: Library 1
D. E. Bode 1
R. M. Talley 1

Shockley Transistor
Unit of Clevite Transistor
391 S. San Antonio Road
Mount View, California
Attn: Library 1

Sperry Gyroscope Company
Great Neck, Long Island, New York
Attn: Engineering Library 1

Texas Instruments Incorporated
Central Research & Engineering
P. O. Box 1079
Dallas 21, Texas
Attn: C. D. Mouser, Technical Information Services 1
J. R. Macdonald 1
Apparatus Division 1

Westinghouse Research Laboratories
Pittsburgh 35, Pennsylvania
Attn: J. M. Fertig, Head, Tech. Information 2
M. Garbuny, Optical Physics Section 1

Westinghouse Electric Corporation
Research Department
Bloomfield, New Jersey
Attn: H. F. Ivey 1
P. Jaffe 1